Electronic Supplementary Material (ESI) for Organic & Biomolecular Chemistry

Supporting Information

Novel *N*-indolylmethyl substituted olanzapine derivatives: Their design, synthesis and evaluation as PDE4B inhibitors

Dhilli Rao Gorja,[a,b] Soumita Mukherjee,[a] Chandana Lakshmi T. Meda,[a] Girdhar Singh Deora,[a] K. Lalith Kumar,[a] Ankit Jain,[a,c] Girish H. Chaudhari,[a,c] Keerthana S. Chennubhotla,[c] Rakesh K. Banote,[c] Pushkar Kulkarni,[a,c] Kishore V. L. Parsa,[a,]* K. Mukkanti,[b] Manojit Pal[a,]*

[a]Institute of Life Sciences, University of Hyderabad Campus, Gachibowli, Hyderabad 500046, India.

[b]Chemistry Division, Institute of Science and Technology, JNT University, Kukatpally, Hyderabad 500072, India.

[c]Zephase Therapeutics Pvt. Ltd (An incubated company at the Institute of Life Sciences), University of Hyderabad Campus, Gachibowli, Hyderabad 500 046, India.

List of contents

Chemistry

General methods: Unless otherwise stated, reactions were performed under nitrogen atmosphere using oven dried glassware. Reactions were monitored by thin layer chromatography (TLC) on silica gel plates (60 F254), visualized with ultraviolet light or iodine spray. Flash chromatography was performed on silica gel (230-400 mesh) using distilled hexane, ethyl acetate, dichloromethane. ^{1}H NMR and ^{13}C NMR spectra were determined in $CDCl_3$ solution by using 400 and 100 MHz spectrometers, respectively. Proton chemical shifts (δ) are relative to tetramethylsilane (TMS, δ = 0.00) as internal standard and expressed in ppm. Spin multiplicities are given as s (singlet), d (doublet), t (triplet) and m (multiplet) as well as bm (broad multiplet). Coupling constants (*J*) are given in hertz. Infrared spectra were recorded on a FT- IR spectrometer. Melting points were determined using melting point apparatus and are uncorrected. MS spectra were obtained on a mass spectrometer (Agilent 6430 Triple Quadrupole LC/MS).

Preparation of 2-Methyl-10-(4-methyl-piperazinyl)-4-prop-2-ynyl-4*H*-3-thia-4,9-diaza-benzo[*f*]azulene (4)[1]

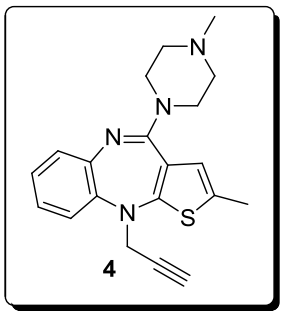

Propargyl bromide (19.2 mmol) was added to a solution of olanzapine (16 mmol) and sodium hydride (32 mmol) in THF (20 mL) under a nitrogen atmosphere. The mixture was stirred at room temperature for 7h. After completion (confirmed by TLC), the mixture was diluted with ice-water (60 mL) and extracted with ethyl acetate (3 x 15 mL). The organic layers were collected, combined, dried over anhydrous Na_2SO_4, filtered and concentrated under low vacuum. The residue was purified by column chromatography using hexane/ethylacetate as eluent to afford the title compound as a white solid (87% yield); mp 155-156 °C; 1H NMR (400 MHz, CDCl3): δ 7.14 (d, *J* = 8.0 Hz, 1H), 7.03-6.91 (m, 3H), 6.32 (s, 1H), 4.24 (bs, 2H), 3.61-3.50 (m, 4H), 2.60-2.45 (bm, 4H), 2.46 (s, 1H), 2.35 (s, 6H); m/z (CI): 351 (M+1, 100%).

General procedure for the preparation of compound 3:

A mixture of compound **4** (1.2 mmol), 10% Pd/C (0.02 mmol), PPh3 (0.15 mmol), CuI (0.03 mmol), and triethylamine (2.40 mmol) in ethanol (5 mL) was stirred at 25–30 °C for 30 min under nitrogen. To this was added o-iodoanilide (**5**) (1.2 mmol), and the mixture was initially stirred at room temperature for 1 h and then at 70 °C for 5 h. After completion of the reaction,

the mixture was cooled to room temperature, diluted with EtOAc (50 mL), and filtered through Celite. The organic layers were collected, combined, washed with water (3 × 30 mL), dried over anhydrous Na_2SO_4, filtered and concentrated under low vacuum. The crude residue was purified by column chromatography on silica gel using methanol/dichloromethane to afford the desired product.

4-(5-Bromo-1-methanesulfonyl-1H-indol-2-ylmethyl)-2-methyl-10-(4-methyl-piperazin-1-yl)-4*H*-3-thia-4,9-diaza-benzo[*f*]azulene (3a)

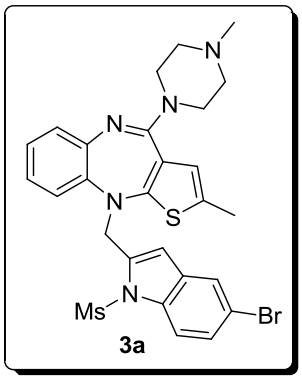

3a

White solid; Yield: 89%; mp 209-211 °C; R_f (10% Methanol/Dichloromethane): 0.52; ^{1}H NMR (400 MHz, $CDCl_3$): δ 7.78 (d, J = 9.2 Hz, 1H), 7.64 (s, 1H), 7.40 (d, J = 8.5 Hz, 1H), 7.08-6.97 (m, 4H), 6.71 (s, 1H), 6.27 (s, 1H), 5.14 (d, J = 15.4 Hz, 1H), 4.88 (d, J = 15.4 Hz, 1H), 3.97-3.81 (bm, 2H), 3.75-3.60 (bm, 2H), 3.15 (s, 3H), 2.99-2.77 (bm, 4H), 2.63 (s, 3H), 2.33 (s, 3H); ^{13}C NMR (100 MHz, $CDCl_3$): δ 157.0, 143.8, 137.0, 135.5, 132.5, 130.3, 127.7, 127.4 (2C), 125.1 (2C), 124.0, 123.7, 121.2, 117.9, 117.0, 115.3 (2C), 112.1, 54.3, 48.2, 45.2 (3C), 41.2, 29.6, 15.8; IR (KBr): 2919, 2848, 2795, 1587, 1367, 1173 cm^{-1}; *m/z* (CI): 598, 600 [M^+, (M + 2), 92%, 100%]; HPLC: 98.6%; column: X Bridge C-18 150*4.6 mm 5µm, mobile phase A: 5 mM NH_4OAc in water, mobile phase B: CH_3CN (gradient) T/B%: 0/50, 2/50, 9/95, 13/95, 15/50, 18/50; flow rate: 1.0 mL/min; UV 225 nm, retention time 9.3 min.

4-(1-Methanesulfonyl-1H-indol-2-ylmethyl)-2-methyl-10-(4-methyl-piperazin-1-yl)-4H-3-thia-4,9-diaza-benzo[*f*]azulene (3b)

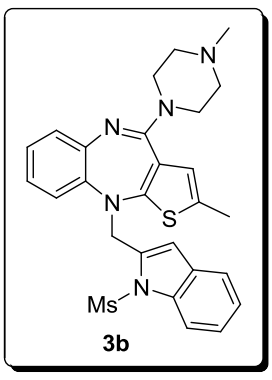

3b

White solid; Yield: 90%; mp 201-203 °C; R_f (10% methanol/dichloromethane): 0.54; ^{1}H NMR (400 MHz, $CDCl_3$): δ 7.93 (d, J = 7.8 Hz, 1H), 7.49 (d, J = 7.0 Hz ,1H), 7.31 (d, J = 7.0 Hz, 1H), 7.29 (d, J = 7.8 Hz, 1H), 6.97-7.13 (m, 4H), 6.77 (s, 1H), 6.28 (s, 1H), 5.17 (d, J = 13.0 Hz, 1H), 4.90 (d, J =13.0 Hz, 1H), 3.80-3.62 (bm, 2H), 3.61-3.46 (bm, 2H), 3.16(s, 3H), 2.79-2.58 (bm, 4H), 2.49 (s, 3H), 2.32(s, 3H); ^{13}C NMR (100 MHz, $CDCl_3$): δ 157.0, 155.8, 144.1, 136.9, 135.7, 132.4, 128.7, 127.3, 124.9 (3C), 124.0, 123.6, 121.1, 120.3, 118.0, 113.8, 113.1,

111.5, 54.1, 48.4, 40.9, 31.9, 29.6, 22.6, 15.8, 14.1; IR (KBr): 2918, 2848, 2795, 1590, 1363 cm^{-1}; m/z (CI): 520 (M+1, 100%); HPLC: 98.7%; column: X Bridge C-18 150*4.6 mm, 5µm, mobile phase A: 5 mM NH_4OAc in water, mobile phase B: CH_3CN (gradient) T/B%: 0/40, 2/40, 8/98, 13/98, 15/40, 18/40; flow rate: 1.0 mL/min; UV 255 nm, retention time 8.4 min.

4-(1-Methanesulfonyl-5-nitro-1H-indol-2-ylmethyl)-2-methyl-10-(4-methyl-piperazin-1-yl)-4H-3-thia-4,9-diaza-benzo[*f*]azulene (3c)

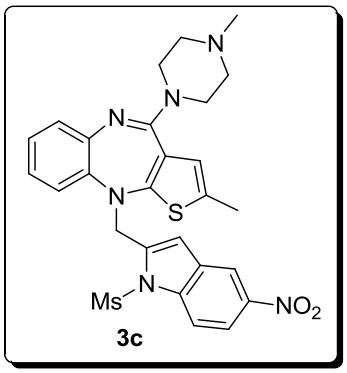

3c

Yellow solid; Yield: 87%; mp 218–219 °C; R_f (10% Methanol/Dichloromethane) 0.56; ^{1}H NMR (400 MHz, $CDCl_3$): δ 8.41 (s, 1H), 8.17 (d, J = 8.8 Hz, 1H), 8.04 (d, J = 9.5 Hz, 1H), 7.15-6.97 (m, 4H), 6.89 (s, 1H), 6.30 (s, 1H), 5.21 (d, J = 15.2 Hz, 1H), 4.93 (d, J = 15.2 Hz, 1H), 3.83-3.57 (bm, 4H), 3.33(s, 3H), 2.96-2.70 (bm, 4H), 2.59 (s, 3H), 2.35(s, 3H); ^{13}C NMR (100 MHz, $CDCl_3$): δ 157.3, 157.1, 151.5, 144.2, 139.7, 138.6, 132.9, 128.2, 127.5, 125.3, 124.4, 121.1, 120.0 (2C), 118.0, 117.3, 114.1 (2C), 113.1, 109.9, 54.3, 48.0, 42.1, 29.6, 22.6, 15.9, 14.0; IR (KBr): 2923, 2851, 1579, 1519, 1369, 1168 cm^{-1}; *m/z* (CI): 565 ([M + 1], 100%); HPLC: 97.6%; column: X Bridge C-18 150*4.6 mm 5µm, mobile phase A: 5 mM NH_4OAc in water, mobile phase B: CH_3CN (gradient) T/B%: 0/40, 2/40, 8/98, 13/98, 15/40, 18/40; flow rate: 1.0 mL/min; UV 255 nm, retention time 8.4 min.

1-Methanesulfonyl-2-[2-methyl-10-(4-methyl-piperazin-1-yl)-3-thia-4,9-diaza-benzo[*f*] azulen-4-ylmethyl]-1H-indole-5-carbonitrile (3d)

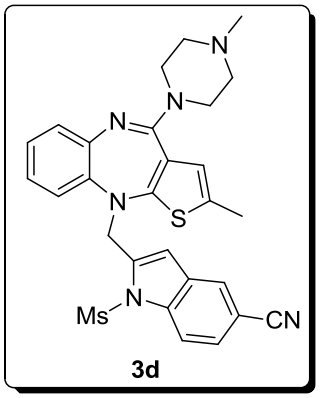

3d

White solid; Yield: 85%; mp 235-236°C; R_f (10% Methanol/Dichloromethane): 0.58; ^{1}H NMR (400 MHz, $CDCl_3$): δ 8.05 (d, J = 8.8 Hz, 1H), 7.83 (s, 1H), 7.54 (d, J = 8.8 Hz, 1H), 7.13-6.96 (m, 4H), 6.81 (s, 1H), 6.30 (s, 1H), 5.20 (d, J = 15.0 Hz, 1H), 4.91 (d, J = 15.0 Hz, 1H), 3.64-3.43 (bm, 4H), 3.31 (s, 3H), 2.76-2.52 (bm, 4H), 2.44 (s, 3H), 2.35 (s, 3H); ^{13}C NMR (100 MHz, $CDCl_3$): δ 157.3, 155.1, 143.5, 138.5, 138.0, 132.5, 128.4, 127.7, 127.4, 125.8, 125.2, 124.0, 121.4, 120.6, 119.1, 117.7, 114.7, 112.0, 111.6, 107.1, 54.8, 48.0, 45.8, 42.0, 29.6, 22.6, 15.9, 14.1; IR (KBr): 2922,

2849, 2796, 2226, 1584, 1369, 1174 cm^{-1}; *m/z* (CI): 544 (M^+, 100%); HPLC: 97.6%; column: X Bridge C-18 150*4.6 mm 5µm, mobile phase A: 5 mM NH_4OAc in water, mobile phase B: CH_3CN (gradient) T/B%: 0/50, 2/50, 9/95, 14/95, 16/50, 18/50; flow rate: 1.0 mL/min; UV 232 nm, retention time 7.1 min.

4-(1-Methanesulfonyl-5-methyl-1H-indol-2-ylmethyl)-2-methyl-10-(4-methyl-piperazin-1-yl)-4H-3-thia-4,9-diaza-benzo[*f*]azulene (3e)

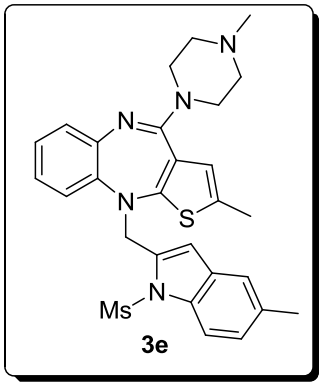

3e

White solid; Yield: 81%; mp 153–156 °C; R_f (10% Methanol/Dichloromethane): 0.67; ^1H NMR (400 MHz, $CDCl_3$): δ 7.83 (d, J = 8.8 Hz, 1H), 7.27 (s, 1H), 7.11 (d, J = 8.8 Hz, 1H), 7.08-6.98 (m, 4H), 6.70 (s, 1H), 6.29 (s, 1H), 5.15 (d, J = 15.2 Hz, 1H), 4.89 (d, J = 15.2 Hz, 1H), 3.60-3.42 (bm, 4H), 3.19(s, 3H), 2.59-2.41(bm, 4H), 2.40 (s, 3H), 2.36 (s, 3H), 2.32 (s, 3H); ^{13}C NMR (100 MHz, $CDCl_3$): δ 157.5, 155.5, 144.1, 143.1, 135.8, 135.1, 133.1, 132.0, 128.9, 127.3, 126.1, 124.9, 123.8, 121.4, 120.8, 117.9, 113.5, 112.5, 109.9, 55.1, 48.4, 46.5, 46.1, 41.0, 30.6, 28.2, 21.1, 15.8; IR (KBr): 2923, 2853, 1584, 1365, 1166 cm^{-1}; *m/z* (CI): 534 ([M + 1], 100%); HPLC: 98.6%; column: X Bridge C-18 150*4.6 mm 5µm, mobile phase A: 0.1 % Formic Acid in water mobile phase B: CH_3CN (gradient) T/B%: 0/50, 2/50, 9/98, 12/98, 15/50, 18/50; flow rate: 1.0 mL/min; UV 222 nm, retention time 8.3 min.

1-{1-Methanesulfonyl-2-[2-methyl-10-(4-methyl-piperazin-1-yl)-3-thia-4,9-diaza-benzo[*f*]azulen-4-ylmethyl]-1H-indol-5-yl}-ethanone (3f)

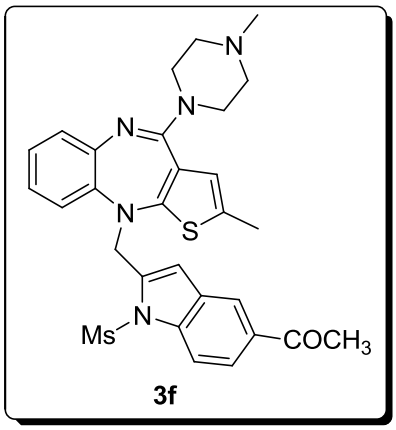

3f

White solid; Yield: 82%; mp 199-201 °C; R_f (10% Methanol/Dichloromethane): 0.58; ^1H NMR (400 MHz, $CDCl_3$): δ 8.15 (s, 1H), 8.02-7.90 (m, 2H), 7.10-6.98 (m, 4H), 6.86 (s, 1H), 6.29 (s, 1H), 5.19 (d, J = 14.4 Hz, 1H), 4.93 (m, 1H), 3.96-3.78 (bm, 2H), 3.78-3.61 (bm, 2H), 3.23 (s, 3H), 2.98-2.72 (bm, 4H), 2.64 (s, 3H), 2.58 (s, 3H), 2.34 (s, 3H); ^{13}C NMR (100 MHz, $CDCl_3$): δ 197.3, 156.8, 155.8, 145.4, 144.4, 139.3, 136.8, 133.0, 128.3, 127.1, 125.1, 125.0, 123.1, 122.2, 120.7, 118.3, 113.7 (2C), 113.6, 109.9, 53.3, 48.1, 44.0, 41.3, 29.5, 26.7, 22.5,

15.8, 14.0; IR (KBr): 2922, 2855, 1676, 1588, 1366, 1165 cm^{-1}; *m/z* (CI): 561 (M^+, 100%); HPLC: 94.1%; column: X Bridge C-18 150*4.6 mm 5µm, mobile phase A: 5 mM NH_4OAc in water, mobile phase B: CH_3CN (gradient) T/B%: 0/70, 2/70, 9/98, 14/98, 15/70, 18/70; flow rate: 1.0 mL/min; UV 210 nm, retention time 3.2 min.

2-Methyl-10-(4-methyl-piperazin-1-yl)-4-[1-(toluene-4-sulfonyl)-1H-indol-2-ylmethyl]-4H-3-thia-4,9-diaza-benzo[*f*]azulene (3g)

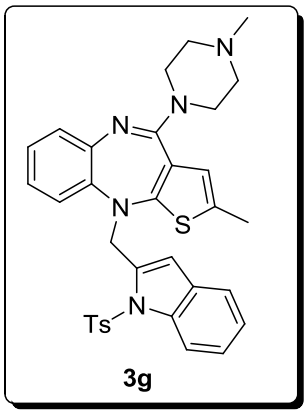

3g

Green solid; Yield: 72%; mp 187-188 °C; R_f (10% Methanol/Dichloromethane): 0.52; ^1H NMR (400 MHz, $CDCl_3$): δ 8.09 (d, *J* = 8.5 Hz, 1H), 7.68 (d, *J* = 8.5 Hz, 2H), 7.34 (d, *J* = 7.6 Hz, 1H), 7.23 (d, *J* = 8.5 Hz, 1H), 7.22-7.14 (m, 3H), 7.07 (d, *J* = 7.6 Hz, 1H), 7.00 (t, *J* = 7.6 Hz, 1H), 6.94 (t, *J* = 7.6 Hz, 1H), 6.88 (d, *J* = 7.6 Hz, 1H), 6.73 (s, 1H), 6.29 (s, 1H), 5.22-4.98 (m, 2H), 3.72-3.51 (bm, 4H), 2.64-2.47 (bm, 4H), 2.39 (s, 3H) 2.33 (s, 3H), 2.27 (s, 3H); ^{13}C NMR (100 MHz, $CDCl_3$): δ 158.8, 155.7, 154.7, 153.4, 145.0, 137.1, 135.5, 132.2, 129.9 (3C), 129.3, 127.3, 126.4 (2C), 124.9, 124.4, 123.9, 123.6, 121.2, 120.8 (2C), 118.0, 114.4, 107.9, 54.3, 49.6, 33.8, 31.9, 22.6, 21.5, 15.8, 14.1; IR (KBr): 2923, 2852, 2792, 1582, 1371, 1176 cm^{-1}; *m/z* (CI): 595 (M^+, 100%); HPLC: 94.5%; column: X Bridge C-18 150*4.6 mm 5µm, mobile phase A: 5 mM NH_4OAc in water mobile phase B: CH_3CN (gradient) T/B%: 0/50, 3/50, 8/98, 15/50, 18/50; flow rate: 1.0 mL/min; UV 220 nm, retention time 9.8min.

4-[5-Chloro-1-(toluene-4-sulfonyl)-1H-indol-2-ylmethyl]-2-methyl-10-(4-methyl-piperazin-1-yl)-4H-3-thia-4,9-diaza-benzo[*f*]azulene (3h)

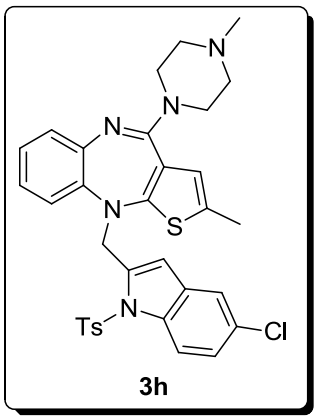

3h

Green solid; Yield: 85%; mp 202-204 °C; R_f (10% Methanol/Dichloromethane): 0.54; ^1H NMR (400 MHz, $CDCl_3$): δ 7.96 (d, *J* = 9.2 Hz, 1H), 7.65-7.58 (m, 2H), 7.31 (s, 1H), 7.22-7.15 (m, 3H), 7.10–6.91 (m, 3H), 6.88 (d, *J* = 7.0 Hz, 1H), 6.66 (s, 1H), 6.28 (s, 1H), 5.12 (m, 1H), 5.02 (m, 1H), 3.98-3.77 (m, 2H), 3.75-3.58 (bm, 2H), 2.82-2.61 (bm, 4H), 2.52 (s, 3H), 2.34 (s, 3H), 2.29 (s, 3H); ^{13}C NMR (100 MHz, $CDCl_3$): δ 157.0, 155.4, 145.3,

144.2, 143.0 (2C), 138.7, 135.4, 135.2, 132.2, 130.5, 130.0 (2C), 129.4, 127.4, 126.4 (2C), 125.0, 124.5, 123.9, 121.3, 118.0, 115.4, 111.1, 109.9, 54.4, 49.6, 45.6, 45.5, 29.6, 21.6, 15.8, 14.1; IR (KBr): 2925, 2849, 2791, 1585, 1375, 1171 cm^{-1}; *m/z* (CI): 629 (M^+, 100%); HPLC: 95.3%; column: X Bridge C-18 150*4.6 mm 5µm, mobile phase A: 5 mM NH_4OAc in water mobile phase B: CH_3CN (gradient) T/B%: 0/80, 2/80, 9/95, 14/95, 15/80, 18/80; flow rate: 1.0 mL/min; UV 225 nm, retention time 6.4 min.

4-[5-Bromo-1-(toluene-4-sulfonyl)-1H-indol-2-ylmethyl]-2-methyl-10-(4-methyl-piperazin-1-yl)-4H-3-thia-4,9-diaza-benzo[*f*]azulene (3i)

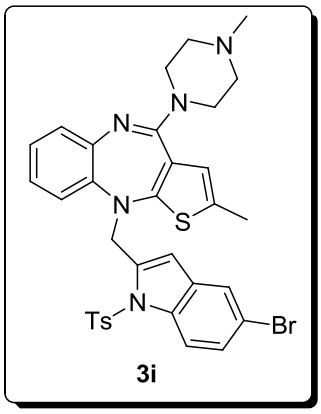

3i

White solid; Yield: 76%; mp 187–189 °C; R_f (10% Methanol/Dichloromethane): 0.58; ^1H NMR (400 MHz, $CDCl_3$): δ 7.86 (d, *J* = 9.2 Hz, 1H), 7.58 (d, *J* = 8.5 Hz, 2H), 7.50 (s, 1H), 7.32 (dd, *J* = 9.2, 1.6 Hz, 1H), 7.19 (d, *J* = 8.5 Hz, 2H), 7.10-6.91 (m, 3H), 6.89 (m, 1H), 6.66 (s, 1H), 6.28 (s, 1H), 5.12 (m, 1H), 5.01 (m, 1H), 4.19-3.89 (bm, 2H), 3.78-3.59 (bm, 2H), 3.00-2.75 (bm, 4H), 2.61 (s, 3H), 2.34 (s, 3H), 2.31 (s, 3H); ^{13}C NMR (100 MHz, $CDCl_3$): δ 156.8, 155.5, 145.3, 144.2, 143.0, 138.5, 135.8, 135.2, 132.3, 131.0, 130.0 (2C), 127.4, 127.3 (2C), 126.4, 125.0, 123.9, 123.4, 121.2, 118.0, 117.1, 115.8, 111.2, 109.9, 54.2, 49.5, 45.7, 45.6, 45.3, 29.6, 21.5, 15.8; IR (KBr): 2977, 2791, 1589, 1373, 1173 cm^{-1}; *m/z* (CI): 674, 676 [M^+, (M + 2), 92.3%, 100%); HPLC: 98.5%; column: X Bridge C-18 150*4.6 mm 5µm, mobile phase A: 5 mM NH_4OAc in water mobile phase B: CH_3CN (gradient) T/B%: 0/85, 2/85, 9/98, 13/98, 15/85, 18/85; flow rate: 1.0 mL/min; UV 220 nm, retention time 5.6 min.

1-[2-[2-Methyl-10-(4-methyl-piperazin-1-yl)-3-thia-4,9-diaza-benzo[*f*]azulen-4-ylmethyl]-1-(toluene-4-sulfonyl)-1H-indol-5-yl]-ethanone (3j)

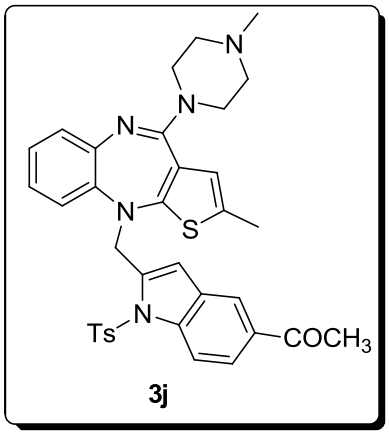

3j

Green solid; Yield: 78%; mp 175-177 °C; R_f (10% Methanol/Dichloromethane): 0.52; ^1H NMR (400 MHz, $CDCl_3$): δ 8.02 (s, 1H), 8.01 (d, *J* = 9.2 Hz, 1H), 7.86 (d, *J* = 9.2 Hz, 1H), 7.60 (d, *J* = 8.0 Hz, 2H), 7.20 (d, *J* = 8.0 Hz, 2H), 7.13-6.97 (m, 3H), 6.93 (d, *J* = 7.0 Hz, 1H), 6.82 (s,

1H), 6.29 (s, 1H), 5.18 (m, 1H), 5.02 (d, J = 12.8 Hz, 1H), 4.27-4.05 (bm, 2H), 3.83-3.67 (bm, 2H), 3.12-2.83 (bm, 4H), 2.69 (s, 3H), 2.59 (s, 3H), 2.33 (s, 3H), 2.32 (s, 3H); ^{13}C NMR (100 MHz, $CDCl_3$): δ 197.5, 157.3, 156.2, 155.7 (2C), 155.2, 145.6, 139.6, 137.9, 136.6, 134.9, 133.2, 130.1 (2C), 128.9, 127.4, 126.4 (2C), 125.2, 124.9, 122.0, 121.0, 120.0, 118.3, 114.3, 53.1, 53.0, 49.1, 44.2, 31.9, 31.6, 29.6, 26.7, 21.6, 15.9; IR (KBr): 2924, 2855, 2579, 1678, 1590, 1371, 1167 cm^{-1}; m/z (CI): 637 (M^+, 100%); HPLC: 94.2%; column: X Bridge C-18 150*4.6 mm 5µm, mobile phase A: 5 mM NH_4OAc in water mobile phase B: CH_3CN (gradient) T/B%: 0/50, 2/50, 9/95, 14/95, 16/50, 18/50; flow rate: 1.0 mL/min; UV 230 nm, retention time 9.2 min.

Possible mechanism for the synthesis of indole ring via Cu-mediated *in situ* cyclisation.

The alkynylation proceeds via generation of an active Pd(0) species, generated from the minor portion of the bound palladium (Pd/C) via a Pd leaching process in the solution.[2] The leached Pd then becomes an active species *in situ* by interacting with phosphine ligands. A soluble Pd(0)–PPh_3 complex then undergoes oxidative addition with **7** to give the organo-Pd(II) species **9**. Once generated, the organo-Pd(II) species **9** then facilitates the stepwise formation of C–C bond via transmetallation with copper acetylide generated *in situ* from CuI and the terminal alkyne **5** followed by reductive elimination of Pd(0) to afford alkynylated derivative **10**. The catalytic cycle therefore works in solution rather than on the surface, and at the end of the reaction, re-precipitation of Pd occurs on the surface of the charcoal. The Cu-mediated intramolecular ring closure of the internal alkyne **10**, obtained via C-C bond forming Sonogashira coupling reaction provides the indole derivative **8**. Notably, the *o*-sulfonamide moiety plays a significant role in the CuI-mediated cyclization reaction.[3]

Scheme 1. Proposed reaction mechanism for Pd/C-mediated construction of indole ring.

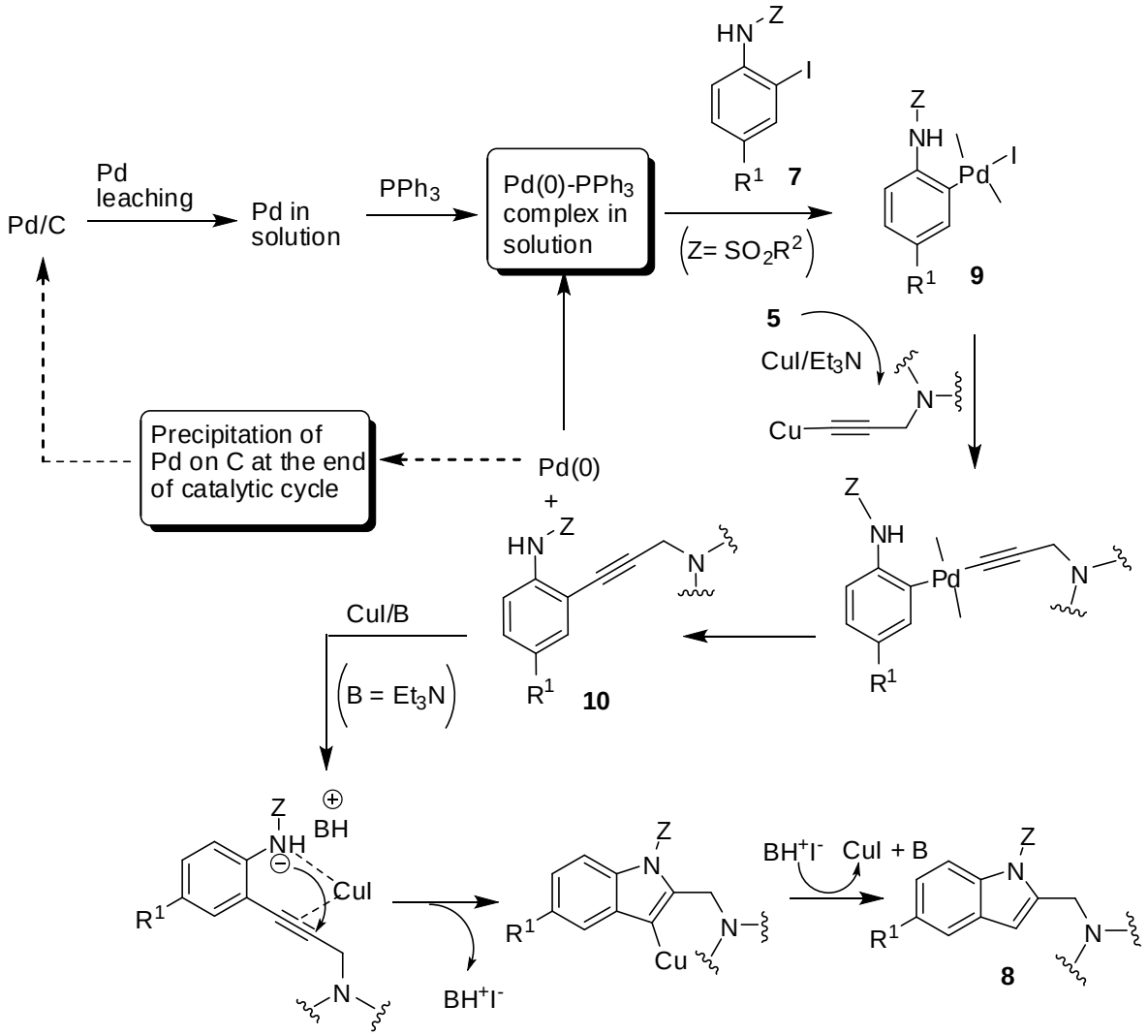

Reference:

1. Fairhurst, J.; Hotten, T. M.; Tupper, D. E.; Wong, D. T. US Patent Application US006034078A, March 7, **2000**.

2. Pal, M. *Synlett* **2009**, 2896–2912.

3. Alinakhi; Prasad, B.; Reddy, U.; Rao, R. M.; Sandra, S.; Kapavarapu, R.; Rambabu, D.; Krishna, G. R.; Reddy, C. M.; Ravada, K.; Misra, P.; Iqbal, J.; Pal, M. *Med. Chem. Commun.* **2011**, *2*, 1006-1010.

Pharmacology

Cells and Reagents: HEK 293T and Sf9 cells were obtained from ATCC (Washington D.C., USA). HEK 293T cells were cultured in DMEM supplemented with 10% fetal bovine serum (Invitrogen Inc., San Diego, CA, USA). Sf9 cells were routinely maintained in Grace's supplemented medium (Invitrogen) with 10% FBS. RAW 264.7 cells (murine macrophage cell line) were obtained from ATCC and routinely cultured in RPMI 1640 medium with 10% fetal bovine serum (Invitrogen Inc.). cAMP was purchased from SISCO Research Laboratories (Mumbai, India). PDElight HTS cAMP phosphodiesterase assay kit was procured from Lonza (Basel, Switzerland). PDElight HTS cAMP phosphodiesterase assay kit was procured from Lonza (Basel, Switzerland). PDE4D2 enzyme was purchased from BPS Bioscience (San Diego, CA, USA). Lipopolysaccharide (LPS) was from *Escherichia coli* strain 0127:B8 obtained from Sigma (St. Louis, MO, USA). Mouse TNF-α ELISA kit was procured from R&D Systems (Minneapolis, MN, USA).

PDE4B protein production and purification

PDE4B cDNA was sub-cloned into pFAST Bac HTB vector (Invitrogen) and transformed into DH10Bac (Invitrogen) competent cells. Recombinant bacmids were tested for integration by PCR analysis. *Sf9* cells were transfected with bacmid using Lipofectamine 2000 (Invitrogen) according to manufacturer's instructions. Subsequently, P3 viral titer was amplified, cells were infected and 48 h post infection cells were lysed in lysis buffer (50 mM Tris-HCl pH 8.5, 10 mM 2-Mercaptoethanol, 1 % protease inhibitor cocktail (Roche), 1 % NP40). Recombinant His-tagged PDE4B protein was purified as previously described in a literature.[1] Briefly, lysate was centrifuged at 10,000 rpm for 10 min at 4 ºC and supernatant was collected. Supernatant was mixed with Ni-NTA resin (GE Life Sciences) in a ratio of 4:1 (v/v) and equilibrated with binding buffer (20 mM Tris-HCl pH 8.0, 500 mM-KCl, 5 mM imidazole, 10 mM 2-mercaptoethanol and 10 % glycerol) in a ratio of 2:1 (v/v) and mixed gently on rotary shaker for 1 hour at 4˚C. After incubation, lysate-Ni-NTA mixture was centrifuged at 4,500 rpm for 5 min at 4˚C and the supernatant was collected as the flow-through fraction. Resin was washed twice with wash buffer (20 mM Tris-HCl pH 8.5, 1 M KCl, 10 mM 2-Mercaptoethanol and 10% glycerol). Protein was eluted sequentially twice using elution buffers (Buffer I: 20 mM Tris-HCl pH 8.5, 100 mM KCl, 250 mM imidazole, 10 mM 2-mercaptoethanol, 10% glycerol, Buffer II: 20 mM Tris-HCl pH 8.5, 100 mM KCl, 500 mM imidazole, 10 mM 2-mercaptoethanol, 10% glycerol). Eluates were collected in

four fractions and analyzed by SDS-PAGE. Eluates containing PDE4B protein were pooled and stored at -80˚C in 50% glycerol until further use.

PDE4B enzymatic assay

The inhibition of PDE4B enzyme was measured using PDElight HTS cAMP phosphodiesterase assay kit (Lonza) according to manufacturer's recommendations. Briefly, 10 ng of PDE4B enzyme was pre-incubated either with DMSO (vehicle control) or compound for 15 min before incubation with the substrate cAMP (5 µM) for 1 h. The reaction was halted with stop solution followed by incubation with detection reagent for 10 minutes in dark. Luminescence values (RLUs) were measured by a Multilabel plate reader (Perkin Elmer 1420 Multilabel counter). The percentage of inhibition was calculated using the following formula and IC_{50}s were computed using GraphPad Prism Version 5.04 software.

$$\%\ inhibition = \frac{(RLU\ of\ vehicle\ control - RLU\ of\ inhibitor)}{RLU\ of\ vehicle\ control} X\ 100$$

PDE4D enzymatic assay

This assay was performed following a similar method as described above using 0.5 ng commercially procured PDE4D2 enzyme instead of 10 ng of in house purified PDE4B without changing any other factors or conditions.

The dose response study curves for compounds **3b** (Fig. 1) and **3c** (Fig. 2) are given below.

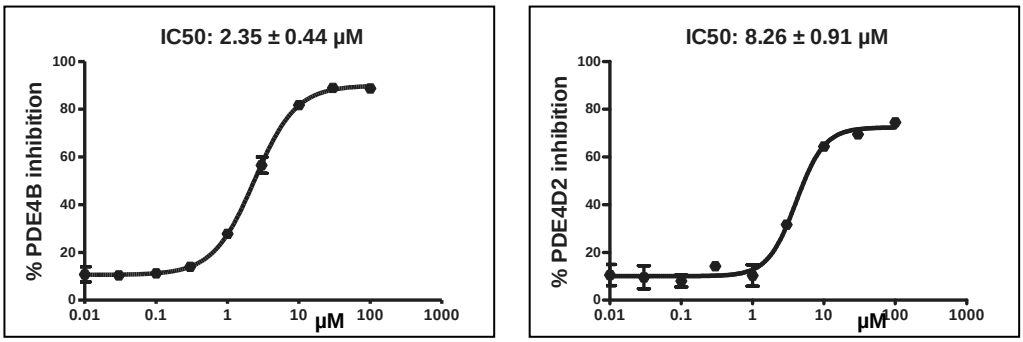

Suppl. Figure 1A. Dose dependent inhibition of PDE4B and PDE4D by compound **3b**.

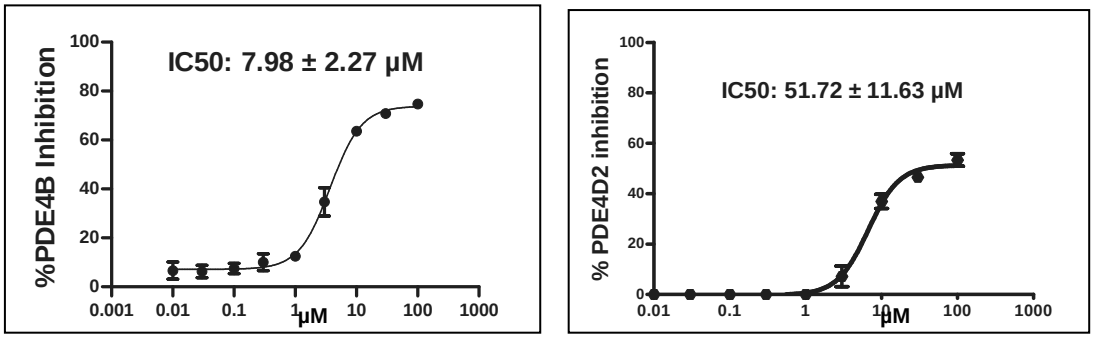

Suppl. Figure 1B. Dose dependent inhibition of PDE4B and PDE4D by compound **3c**.

Cell viability assay

Here, cells were seeded in a 24 well plate, allowed to adhere and then incubated with compounds at 30 µM for 24 h. Post incubation, cells were harvested; 10 µl cell suspension was mixed with 10 µl of 0.4% trypan blue solution and immediately cells were counted under a microscope using a hemocytometer. Live cells were counted by exclusion of trypan blue and are expressed as percentage of total cell count.

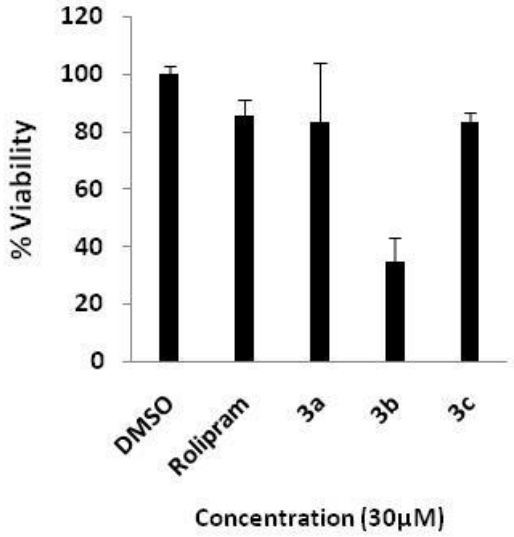

Suppl. Figure 2. Evaluation of cytotoxicity induced by compounds **3a-c** in HEK 293Tcells

TNF-α production assay

For assaying the effect of compounds on TNF-α production, RAW 264.7 cells were pre-incubated either with DMSO (vehicle control) or compound for 30 minutes and then stimulated with 1 µg/ml of LPS overnight. Post-stimulation, cell supernatants were harvested, centrifuged to clear cell debris and the amount of TNF-α in the supernatants was measured using mouse TNF-α DuoSet ELISA kit from R&D Systems according to manufacturer's recommendations. The percentage of inhibition was calculated using the following formula:

$$\% \text{ inhibition} = 100 - \left[\frac{(\text{ LPS stimulated}_{\text{compound}} - \text{unstimulated})}{(\text{LPS stimulated}_{\text{DMSO}} - \text{unstimulated})} \text{ X } 100\right]$$

Reference:

1. Wang, P.; Myers, J. G.; Wu, P.; Cheewatrakoolpong, B.; Egan, R. W.; Billah, M. M. *Biochem. Biophys. Res. Commun.* **1997**, *19*, 320.

Docking study

Method: Docking simulations of molecules were performed using Maestro[1] module implemented from Schrödinger software suite 2011 (version 9.2). The molecules were sketched in 3D format using build panel and LigPrep[2] module was used to produce low-energy conformers. The protein coordinates for docking studies were retrieved from protein data bank with PDB ID: 3O0J (PDE4B) and 1Y2B (PDE4D) [3].* The proteins were prepared by giving preliminary treatment like adding hydrogen, adding missing residues, refining the loop and finally minimized by using OPLS-2005 force fields. Grids for molecular docking were generated by selecting the co-crystal ligands and extended up to 20 Å. The hydroxyl groups of search area were kept flexible during grid generation process.

Compounds were docked using Glide[4] in extra-precision mode, with up to three poses saved per molecule. Ligands were kept flexible by producing the ring conformations and by penalizing non-polar amide bond conformations, whereas the receptors were kept rigid throughout the docking studies. All other parameters of the Glide module were maintained at their default values. For docking method validation, the co-crystal ligands 3OJ (PDB: 3O0J) and DEE (PDB: 1Y2B) were re-docked at the binding sites of their respective proteins and, the obtained docked pose were similar to the reported orientation as well as with minimum RMSD deviation with comparison to bound co-crystal ligands. Similarly, the reference compound rolipram was also docked in the acitive site of PDE4B and 4D. The docking results of compound **3a**, **3b** and **3c** with PDE4B and PDE4D are given in table 1.

*There is no structurally similar (with synthesized molecules) co-crystal ligand reported. So, the crystal structures for PDE4B and PDE4D were chosen on the basis of their high resolution (1.95 Å for 3O0J and 1.40 Å for 1Y2B).

Table 1. Glide score and contributing XP parameters.

Compound	Glide score		LipophilicEvdW		PhobEn		Electro		Penalties	
	PDE4B	PDE4D	PDE4B	PDE4D	PDE4B	PDE4D	PDE4B	PDE4D	PDE4B	PDE4D
3a	-5.11	-2.98	-5.2	-3.61	-0.7	-0.8	-0.2	-0.1	1	1.5
3b	-5.47	-2.90	-4.89	-5.15	-0.99	-0.15	-0.59	-0.1	1	2.5
3c	-5.10	-2.52	-4.22	-5.65	-0.39	-0.42	-0.48	-0.41	0	4
Rolipram	-6.66	-5.0	-4.15	-4.56	-1.09	-1.55	-0.32	-0.72	1.55	1.9

LipophilicEvdW - Chemscore lipophilic pair term and fraction of the total protein-ligand vdw energy.
PhobEn - Hydrophobic enclosure reward.
Electro-Electrostatic reward.
Penalties- Polar atom burial and desolvation penalties, and penalty for intra-ligand contacts.

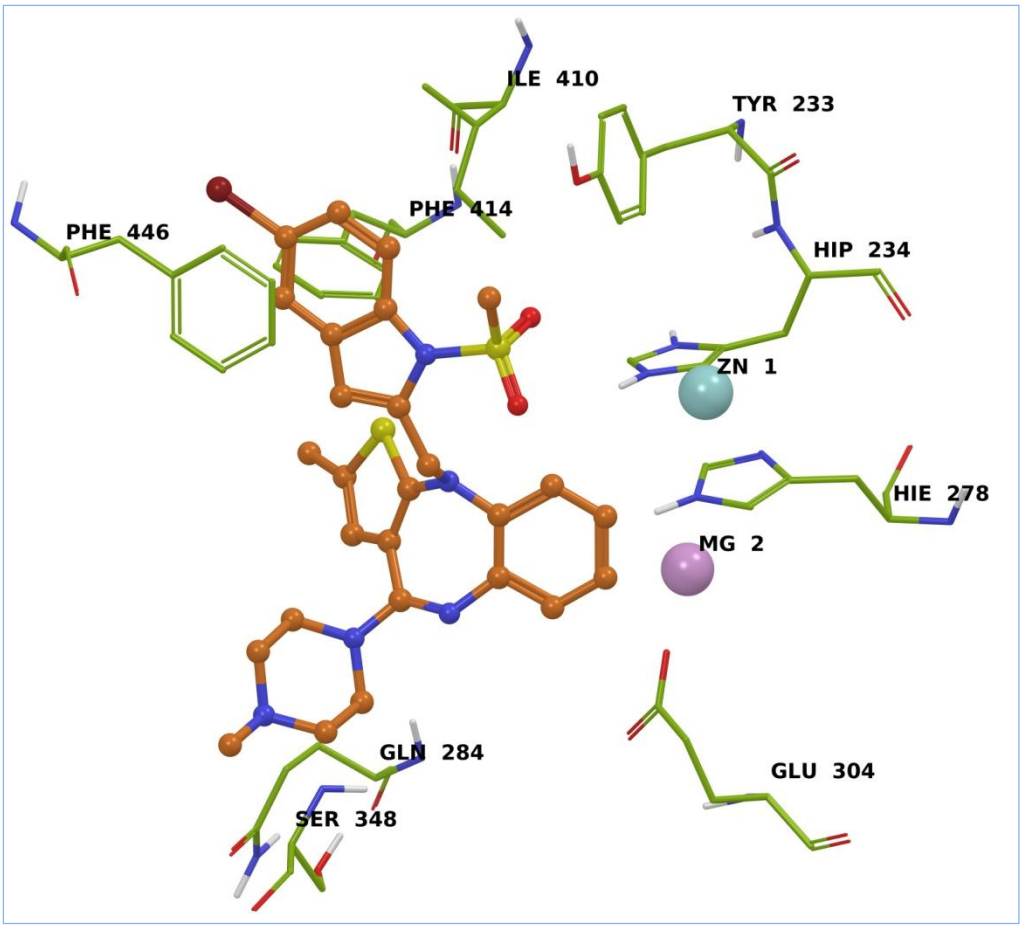

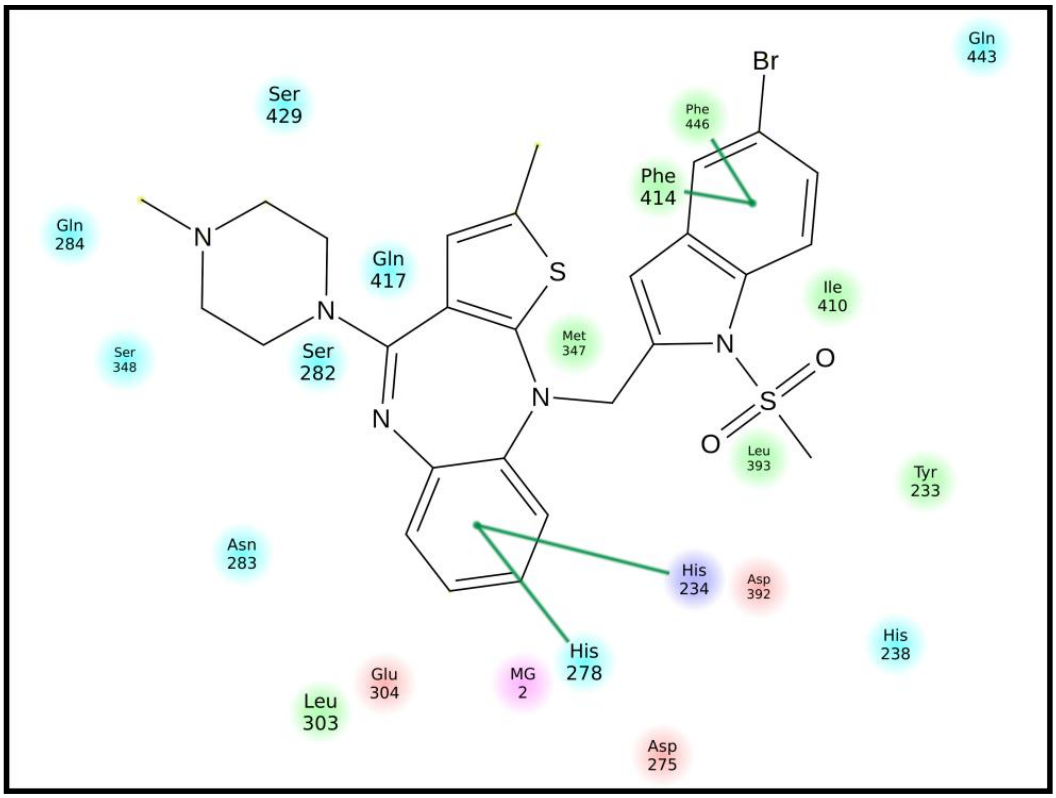

Suppl. Figure 3. Binding mode and interactions of **3a** at the active site of PDE4B.

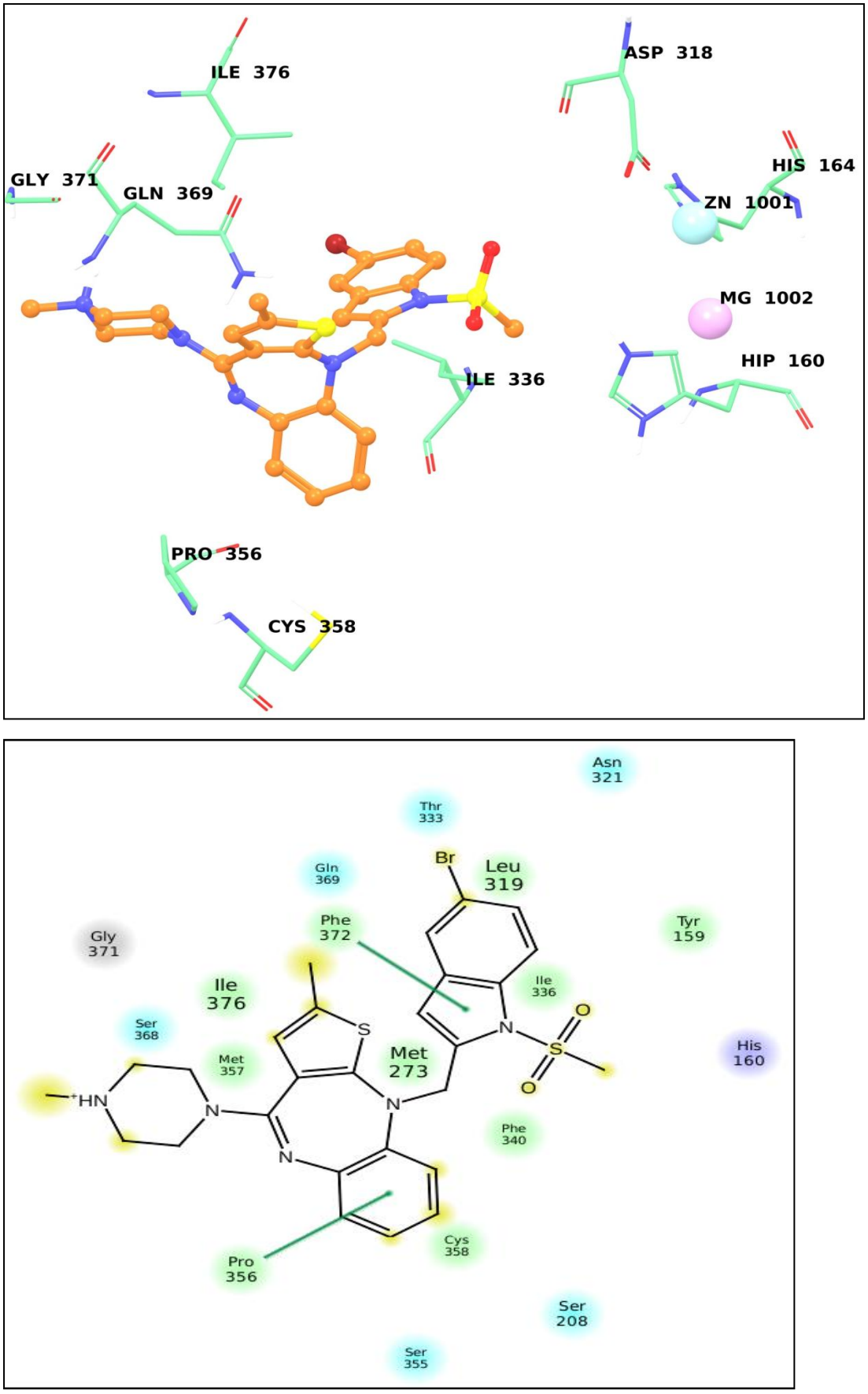

Suppl. Figure 4. Binding mode and interactions of **3a** at the active site of PDE4D.

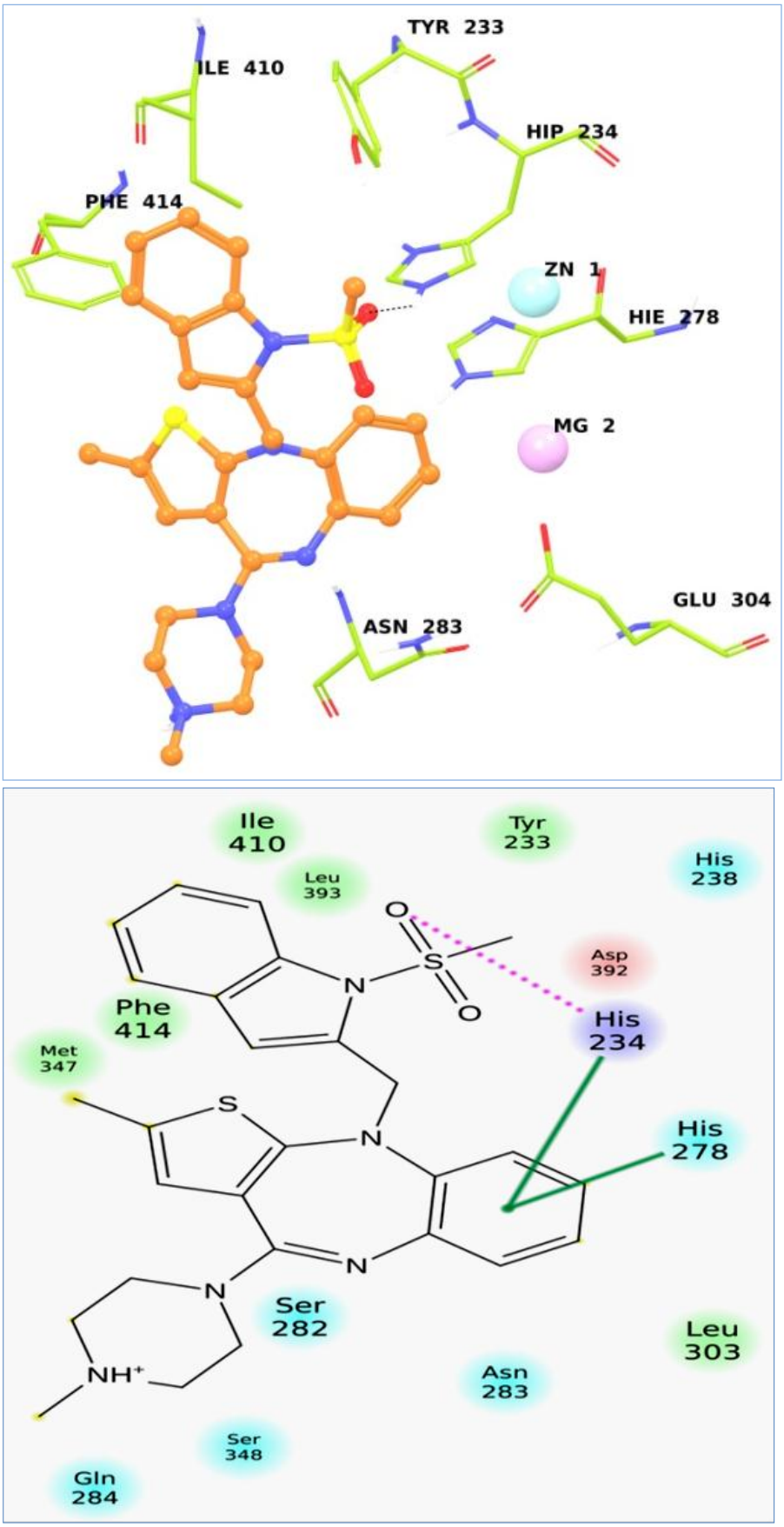

Suppl. Figure 5. Binding mode and interactions of **3b** at the active site of PDE4B.

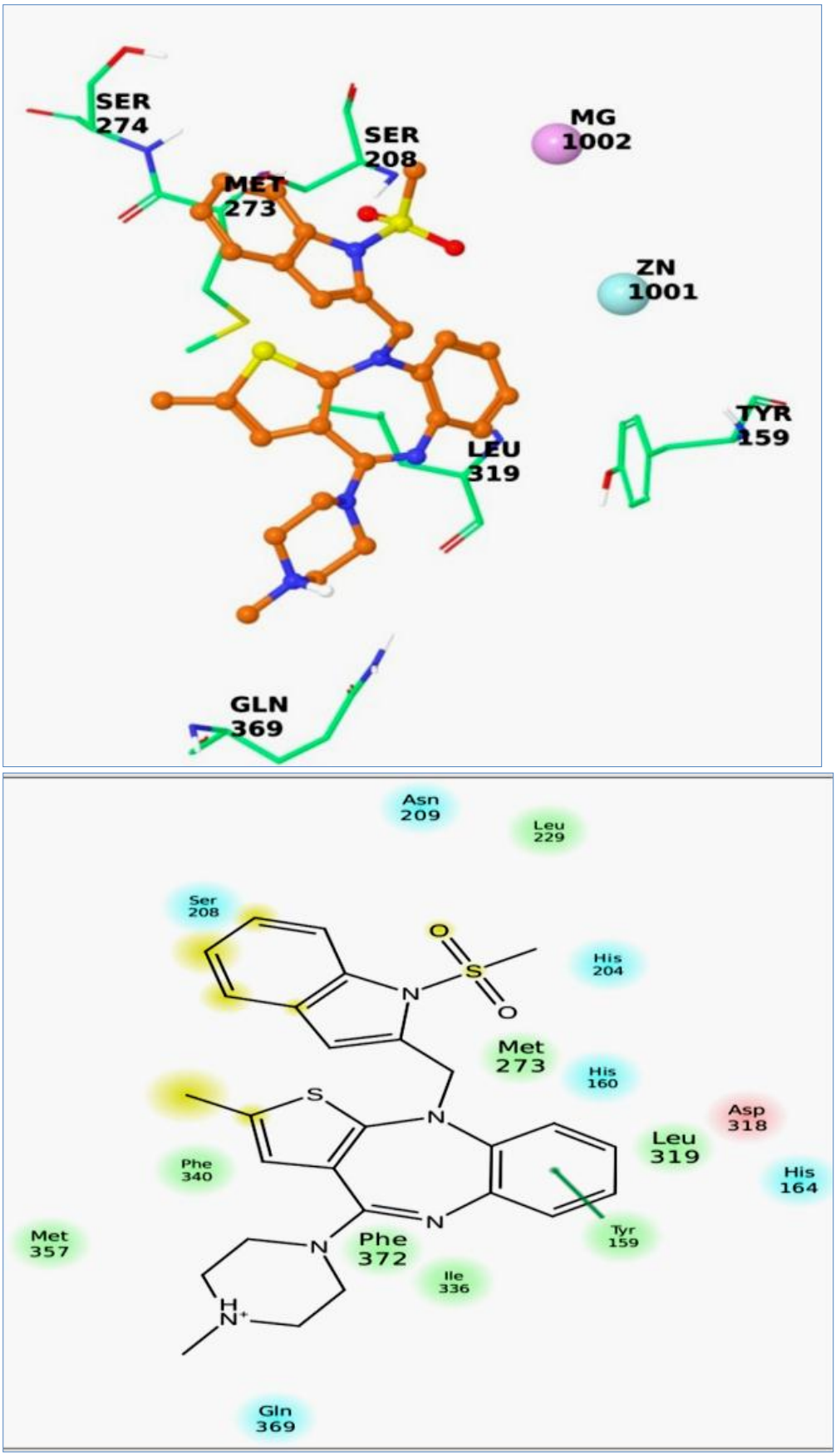

Suppl. Figure 6. Binding mode and interactions of **3b** at the active site of PDE4D.

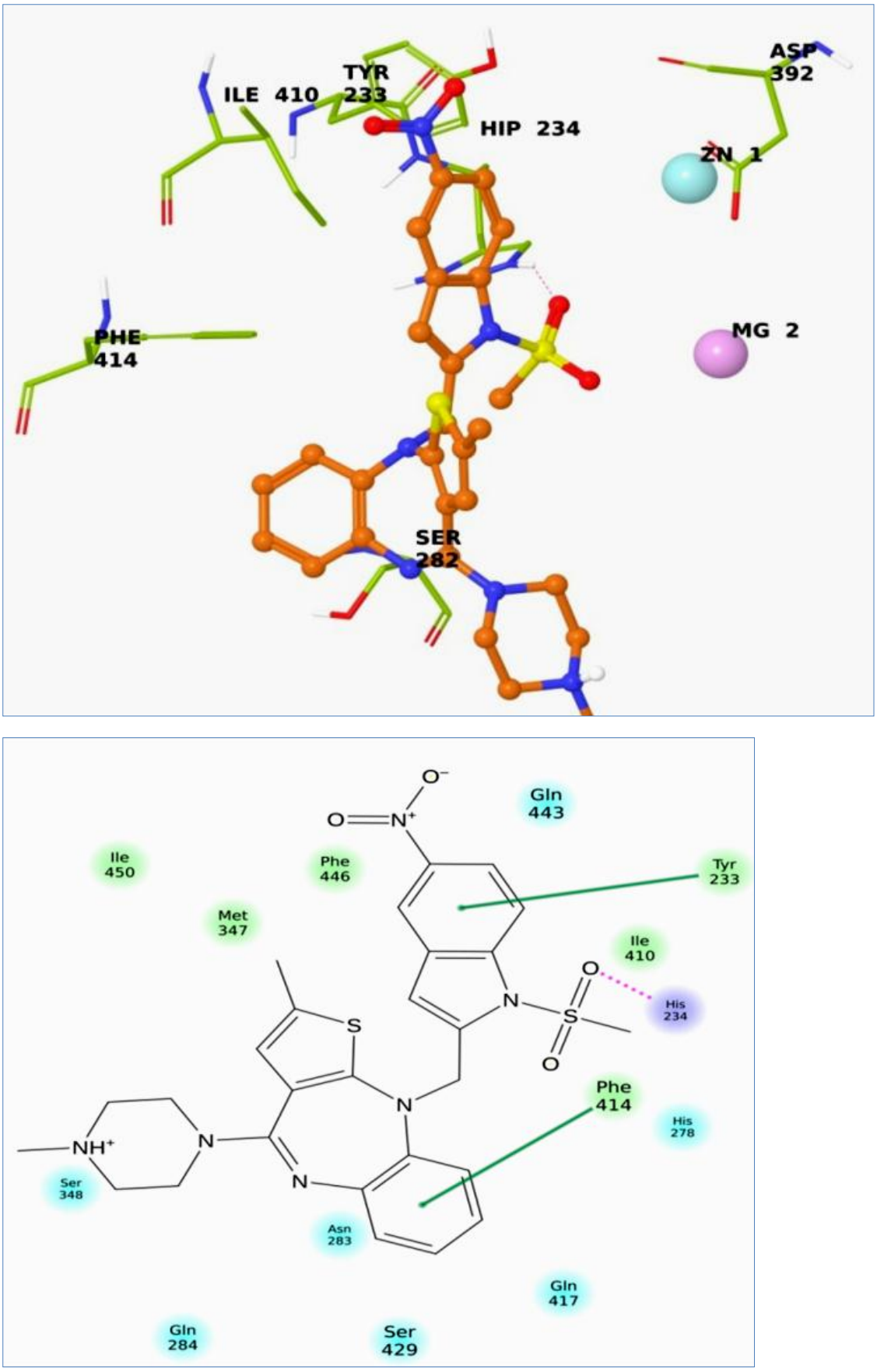

Suppl. Figure 7. Binding mode and interactions of **3c** at the active site of PDE4B.

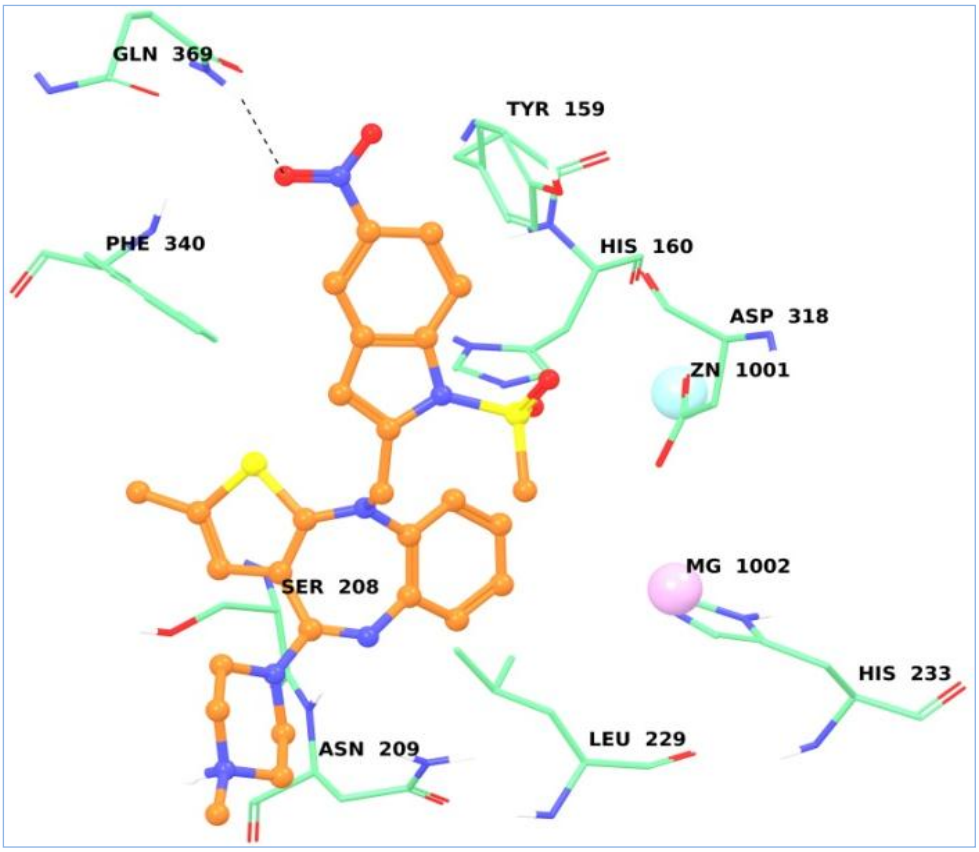

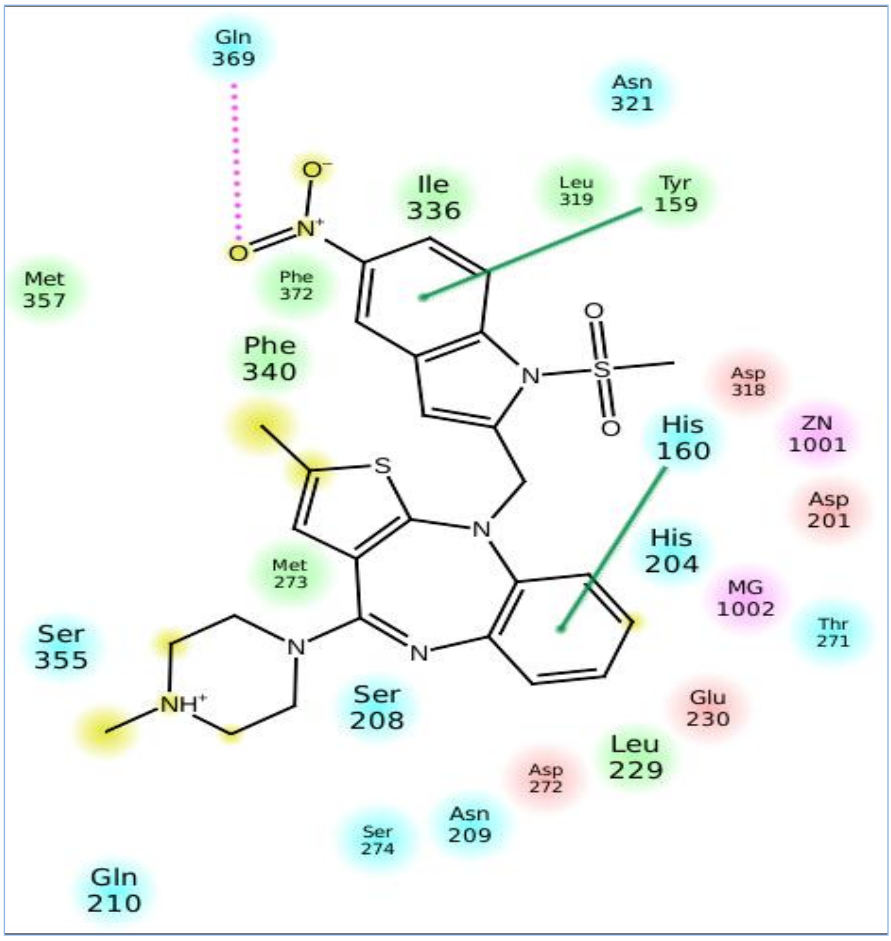

Suppl. Figure 8. Binding mode and interactions of **3c** at the active site of PDE4D.

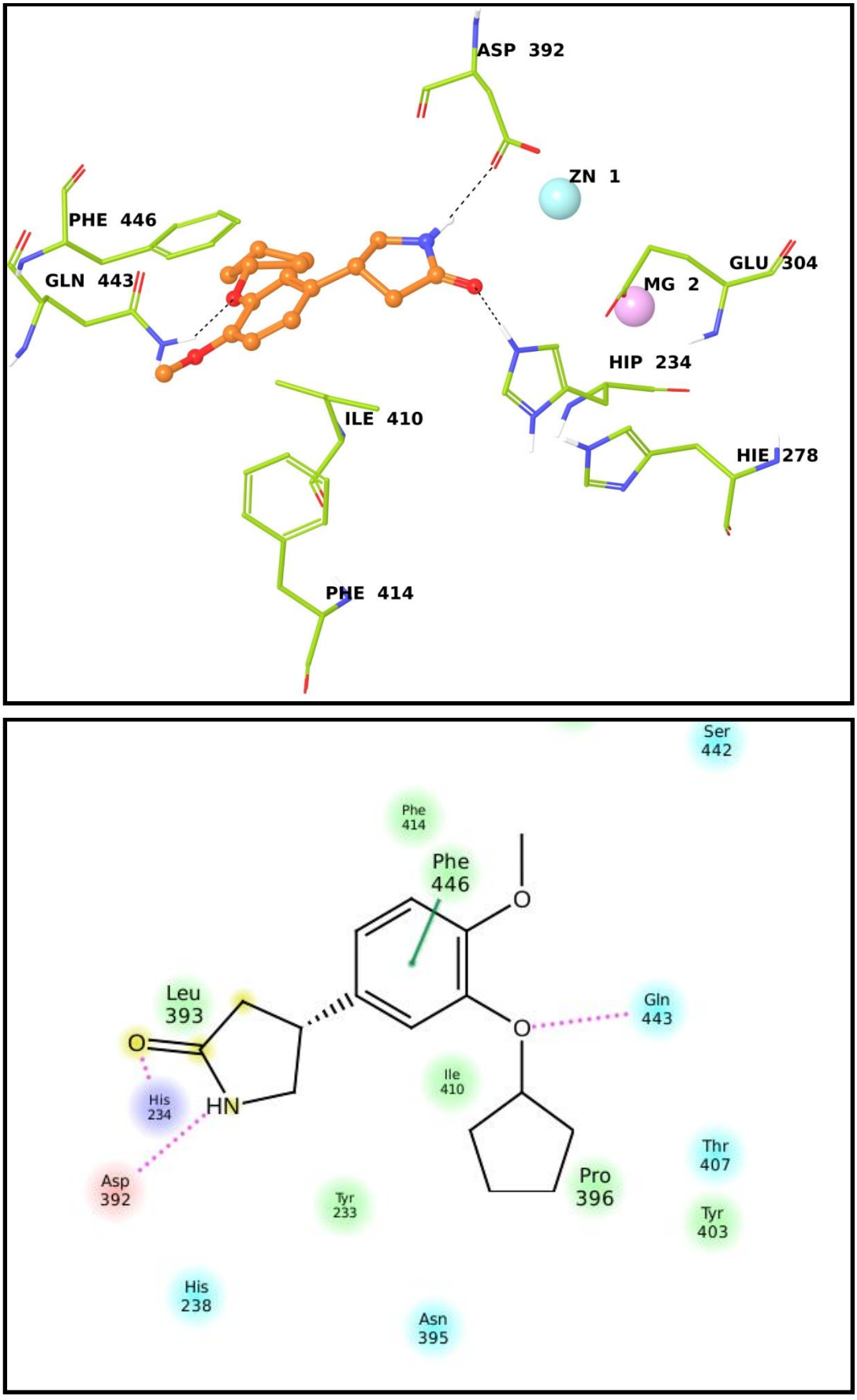

Suppl. Figure 9. Binding mode and interactions of rolipram at the active site of PDE4B.

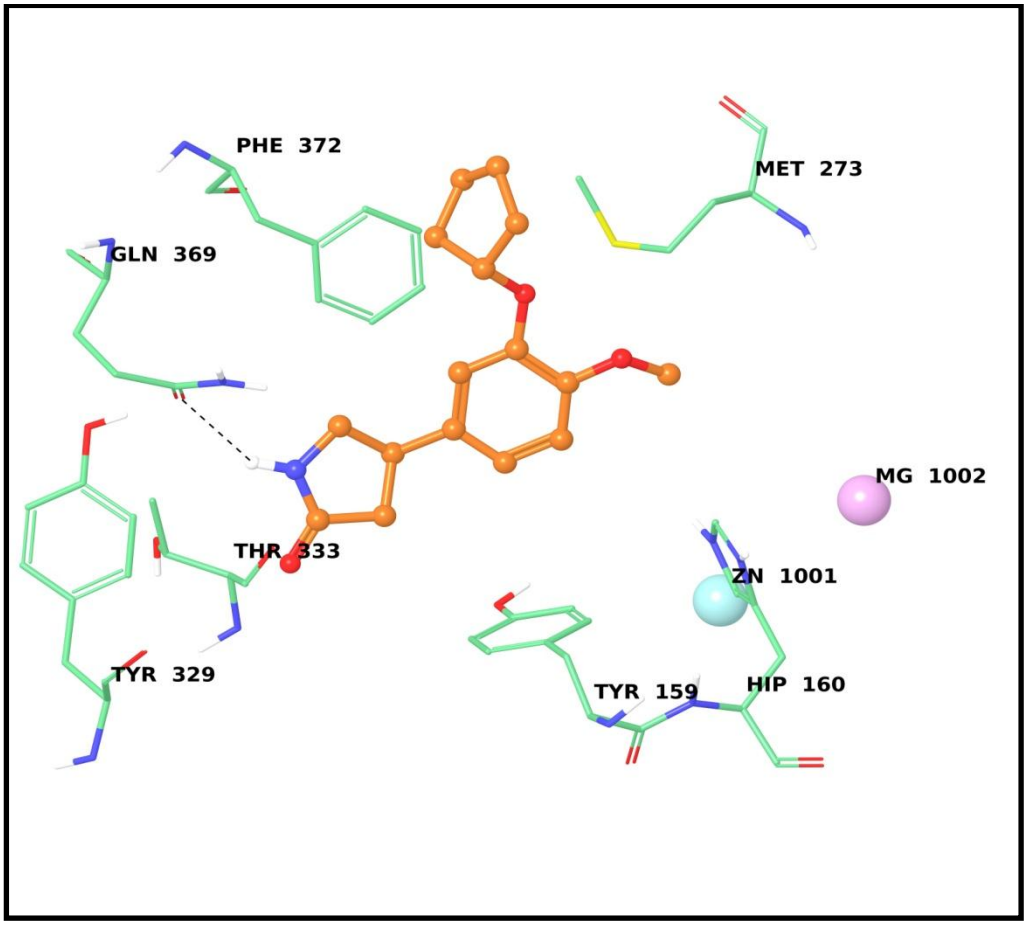

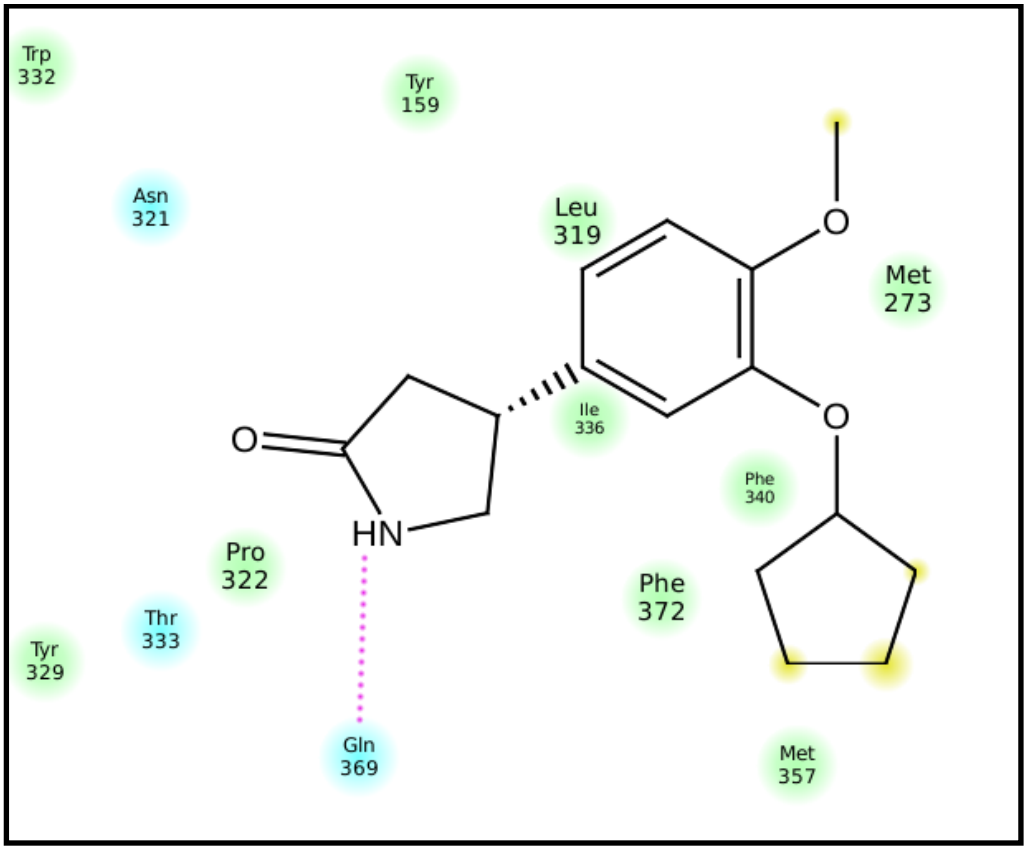

Suppl. Figure 10. Binding mode and interactions of rolipram at the active site of PDE4D.

Docking of **3a** into the PDE4B showed four π-π stacking interactions consisting of (i) two interactions involving phenyl ring (of indole) with Phe 414 and 446 and (ii) other two involving the phenyl ring (of olanzapine moiety) with His 234 and His 278 residues of the PDE4B protein (suppl. Fig. 3). Whereas docking of **3a** with the PDE4D showed π-π stacking interactions between (i) the phenyl ring (of olanzapine moiety) and Pro 356 and (ii) the indole ring and Phe 372 (suppl. Fig. 4). Similarly, docking of **3b** revealed (i) a H-bonding between the oxygen of sulfonyl group and His 234 and (ii) π-π stacking interaction between phenyl ring (of olanzapine moiety) and His 234 and 278 residues of the PDE4B protein (see suppl. Fig. 5 in SI) whereas only one π-π stacking interaction was observed between the benzene ring of olanzapine moiety and Tyr 159 residue (suppl. Fig. 6 of SI) when docked into the PDE4D. The interaction of compound **3c** with the PDE4B protein (suppl. Fig. 7 of SI) was mainly contributed by (i) a H-bond between oxygen of $-SO_2CH_3$ group and -NH of His 234, (ii) a π-π stacking interaction between phenyl ring (of indole) and Tyr 233 and other between phenyl ring (of olanzapine) and Phe 414. The interaction with PDE4D was contributed by H-bond between oxygen of $-NO_2$ and -NH group of Gln 369 and two π-π stacking interactions between two phenyl rings with His 160 and Tyr 159 residues of PDE4D protein (suppl. Fig. 8 of SI).

References:

1. Maestro, version 9.2; Schrodinger, LLC: New York, NY, 2012.
2. Graeme L. Card, Bruce P. England, Yoshihisa Suzuki, Daniel Fong, Ben Powell, Byunghun Lee, Catherine Luu, Maryam Tabrizizad, Sam Gillette, Prabha N. Ibrahim, Dean R. Artis, Gideon Bollag, Michael V. Milburn, Sung-Hou Kim, Joseph Schlessinger, Kam Y.J. Zhang, Structural Basis for the Activity of Drugs that Inhibit Phosphodiesterases. Structure, 12 (12), 2004, 2233-2247, DOI:10.1016/j.str.2004.10.004.
3. MacroModel, version 9.9, Schrödinger, LLC, New York, NY, 2011.
4. Glide, version 5.7; Schrodinger, LLC: New York, NY, 2012.

Homology modeling of catalytic site of human D2 dopamine receptor:

The primary sequence of human D2 dopamine receptor (Uniprot ID: P14416) was retrieved from Uniprot protein knowledgebase. N-terminal was excised from the sequence, as we focused our modeling on seven transmembrane helices and binding pocket. The homology

model was developed on the basis human dopamine D3 receptor in complex with elictopride (PDBID: 3PBL) obtained from the results of NCBI-BLAST.[1] MODELLER version 9.10[2,3] was used to build homology model of human D2 receptor using the structural co-ordinates of human D3 receptor sequence. The sequence alignment of human D2 and D3 receptor showed 50 % identity in sequence. The disulfide bridge between residue cysteine 107 and cysteine 182 were included during homology modeling. The best model was selected based on the stereochemical quality assessed by PDBsum, a web based tool for PROCHECK from website http://www.ebi.ac.uk/thornton-srv/databases/pdbsum/Generate.html. The homology model shows 88.4% residues in most favoured region.

Docking: The docking analysis of molecules was performed using Maestro, version 9.2[4] implemented from Schrödinger molecular modeling suite. All molecules were sketched in 3D format using build module of maestro and minimized through Macromodel to produce low-energy conformers. The modelled protein was energy minimized by using OPLS-2005 force field. The grid for molecular docking was generated with copied co-crystal ligand (elictopride) from the template. Molecules were docked using Glide in extra-precision mode,[5] generating three poses per molecule. The ligands were kept flexible by producing the ring conformations and by penalizing non-polar amide bond conformations, whereas the receptors were kept rigid throughout the docking studies. The lowest energy conformations were selected and, the ligand interactions (docking score, hydrogen bonding and hydrophobic interaction) with target protein were determined.

The respective docking scores are shown in Table 1.

Table 1

Compound	GScore	LipophilicEvdW	PhobEn	HBond	Electro	LowMW	Sitemap	Phobic penal	Penal
Olanzapine	-7.8	-5.1	-1.57	-0.68	-0.08	-0.45	0	0	0
3a	-6.6	-5.5	-0.75	0.00	-0.15	0	-0.4	0.18	0
3b	-6.5	-5.4	-0.75	0.00	-0.18	0	-0.4	0.18	0
3c	-5.7	-5.6	-0.77	0.00	-0.12	0	-0.4	0.11	1

LipophilicEvdW: Chemscore lipophilic pair term and fraction of the total protein-ligand vdw energy
PhobEn: Hydrophobic enclosure reward
HBond: Rewards for hydrogen bonding interaction between ligand and protein
Electro: Electrostatic reward
LowMW:Reward for ligands with low molecular weight
Sitemap: ligand to receptor non-H bonding polar/hydrophobic and hydrophobic/hydrophilic complementarily
Phobic penal: penalty for solvent exposed ligand groups
Penal: polar atom burial and desolvation penalties and penalty for intra-ligand contacts

In silico investigation of binding mode of compounds **3a, 3b** and **3c** in human D2 dopamine receptor revealed differences, when compared to binding mode of olanzapine. In case of olanzapine the nitrogen at 4th position of piperazine ring was involved in forming a H-bond with the side-chain hydroxyl group of Tyr 408 (Fig. 11). On the other hand, compounds **3b** and **3c** make H-bond interaction with the side-chain hydroxyl group of Thr 412 through the sulfonyl group present on the indole moiety. In addition, all three molecules showed pi-pi stacking interaction with Phe 410 through phenyl ring (Fig. 12, 13 and 14). All three molecules almost aligned in the same orientation at the binding site of protein. Olanzapine makes pi-pi stacking interactions with His 393 and Phe 389 through phenyl and thiophenyl ring. In spite of being analogues of olanazapine these molecules showed different orientation of binding than Olanzapine at the active site due to their larger molecular volume thereby lower docking scores compared to olanzapine (Table 1).

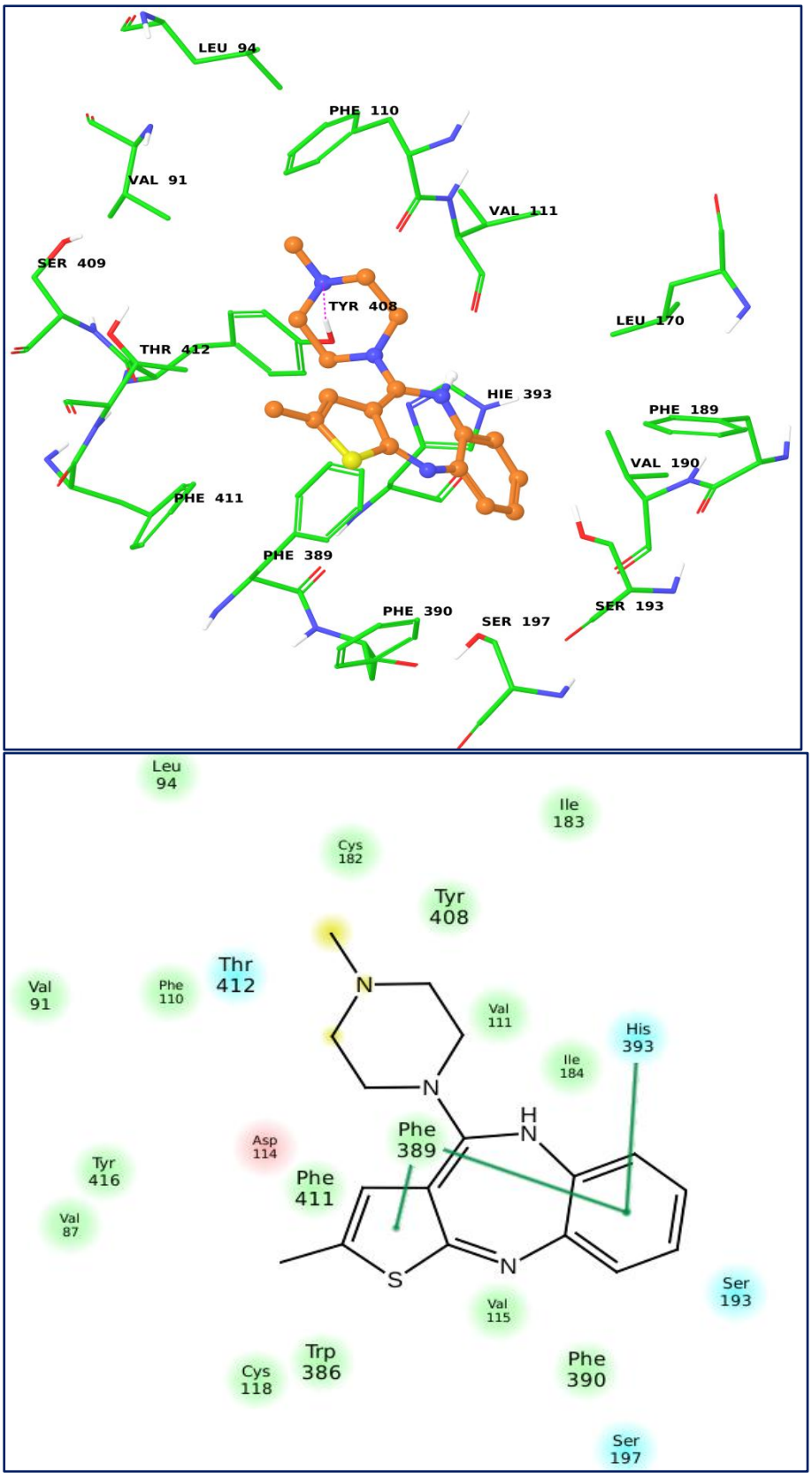

Suppl. Figure 11: Binding mode of olanzapine at the active site of human D2 dopamine receptor.

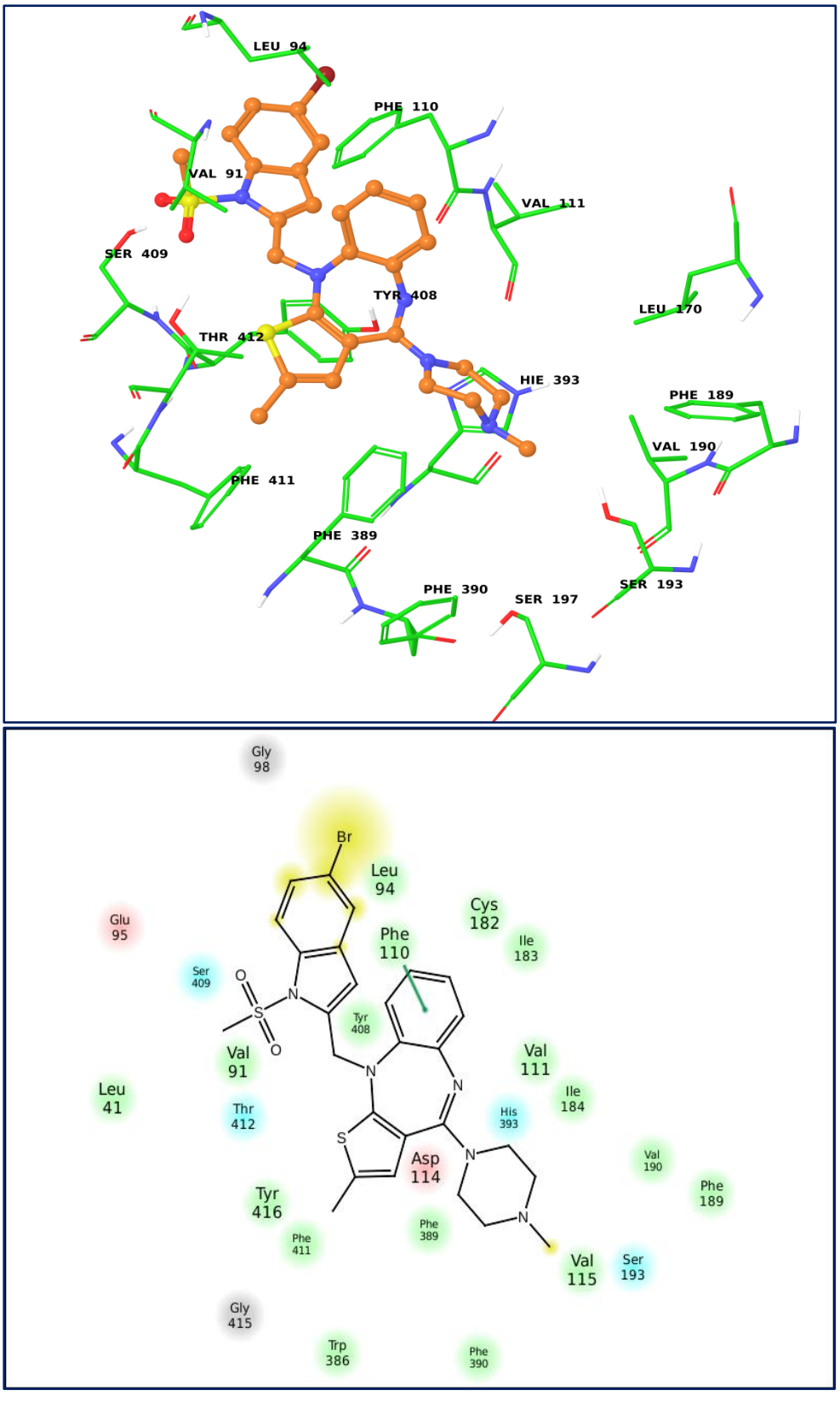

Suppl. Figure 12: Binding mode of **3a** at the active site of human D2 dopamine receptor.

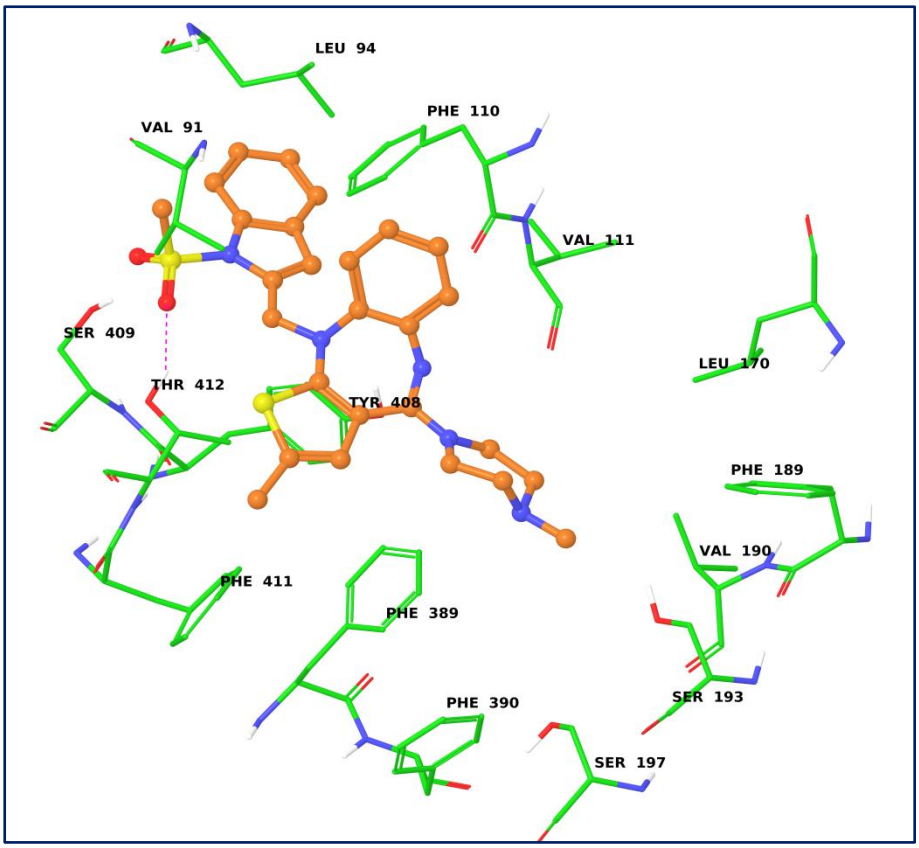

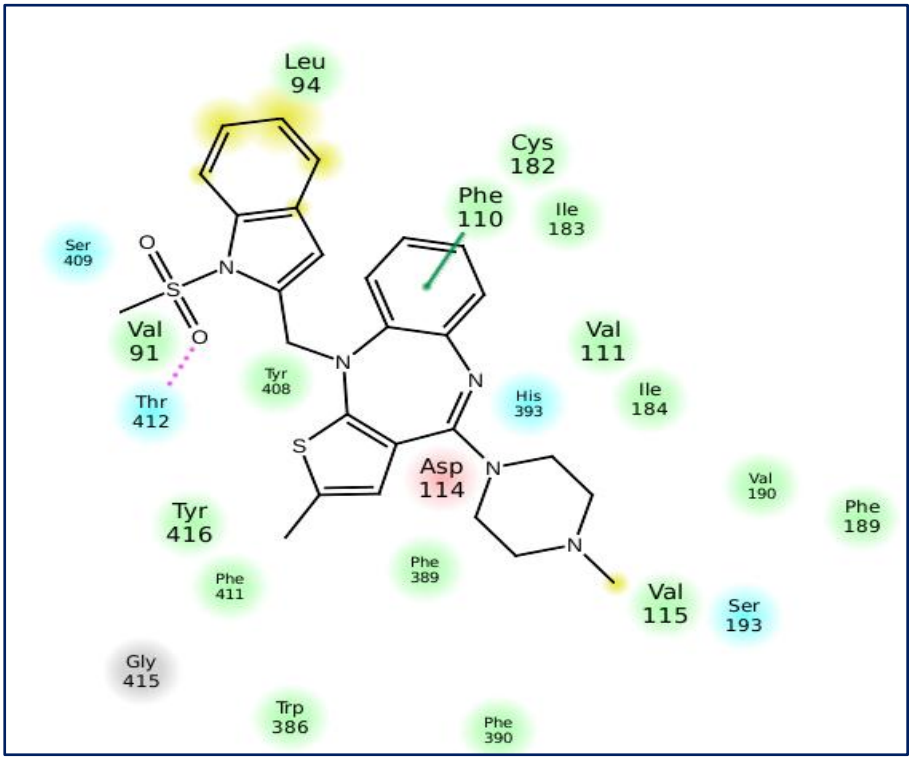

Suppl. Figure 13: Binding mode of **3b** at the active site of human D2 dopamine receptor.

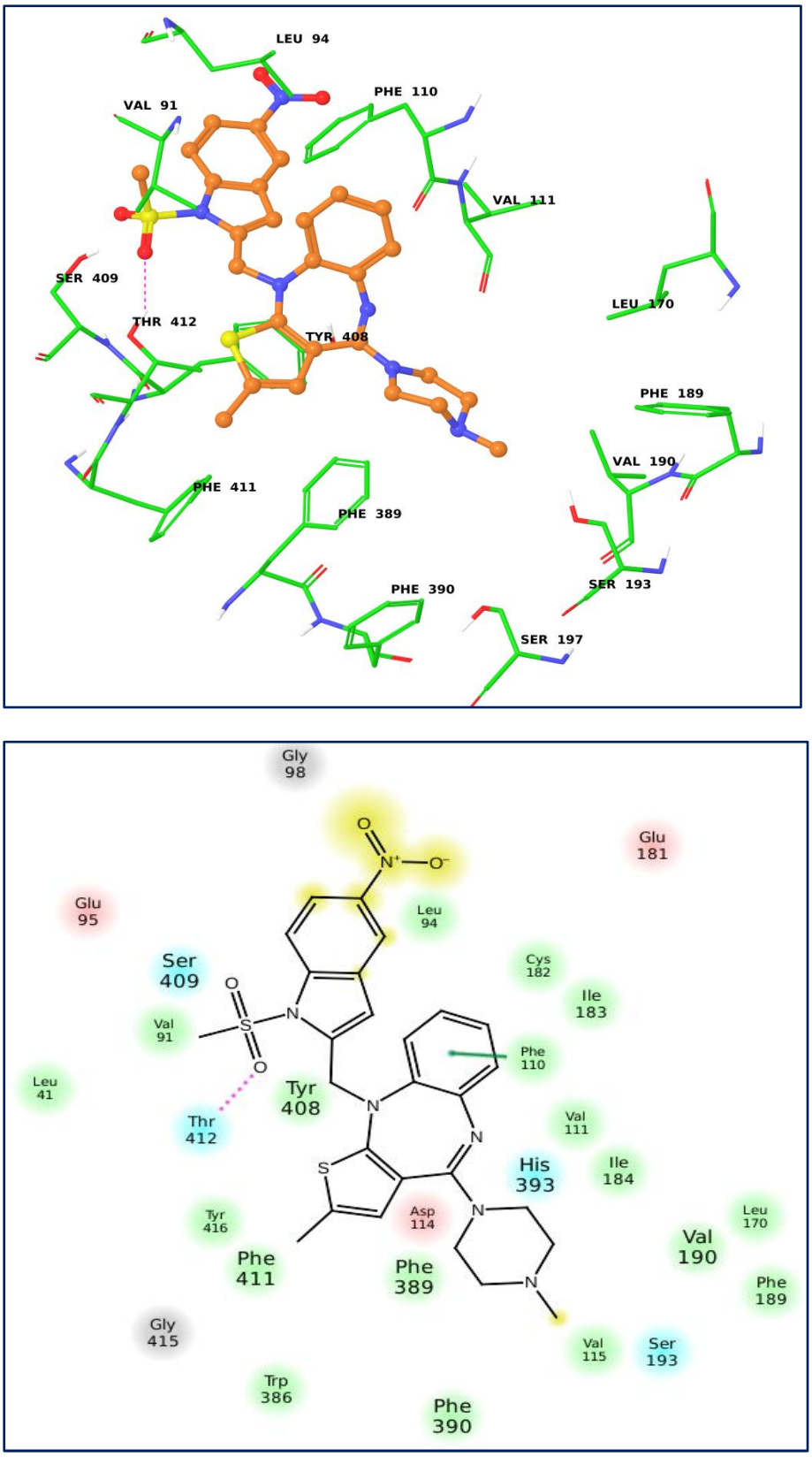

Suppl. Figure 14: Binding mode of **3c** at the active site of human D2 dopamine receptor.

References:

1. S.F. Altschul, T.L. Madden, A.A. Schaffer, J.H. Zhang, Z. Zhang, W. Miller, D.J. Lipman. Gapped BLAST and PSI-BLAST: a new generation of protein database search programs. Nucleic Acids Res., 25 (1997), 3389–3402
2. N. Eswar, M. A. Marti-Renom, B. Webb, M. S. Madhusudhan, D. Eramian, M. Shen, U. Pieper, A. Sali. Comparative Protein Structure Modeling With MODELLER. Current Protocols in Bioinformatics, John Wiley & Sons, Inc., Supplement 15, 5.6.1-5.6.30, 2006
3. A. Sali & T.L. Blundell. Comparative protein modelling by satisfaction of spatial restraints. J. Mol. Biol. 234, 779-815, 1993
4. Maestro, version 9.2; Schrodinger, LLC: New York, NY, 2011
5. Glide, version 5.7; Schrodinger, LLC: New York, NY, 2011

Zebrafish Toxicity Assay methods:

Zebrafish embryos (1 dpf) were dechorinated with Protease (500µg/ml, Sigma Chemicals) for Teratogenicity assay. For hepatotoxicity embryos of 4 dpf were exposed with test molecules and observed on 7dpf. Embryos of 7dpf were exposed for four hours for pro-arrhythmic effect of test compounds. Hepatotoxicity, Teratogenicity, and pro-arrhythmic assays were conducted using the protocols developed by Hill A, Kelly *et al*., and Milan *et al*., respectively. Rolipram was used as a standard drug and three test compounds viz., 3a, 3b and 3c were tested. In teratogenicity cumulative scoring was performed with 90 being total score (18 observation, maximum score of 5 per observation). Data is analyzed and plotted using GraphPad Prism version 5.04 software.

Organs/Systems showing morphological defects				
Treatment	**Concentration**	**Minor**	**Moderate**	**Severe**

	(μM)			
Control	-	None	None	None
Rolipram	10	Tail, Fins, Brain, Facial Structures, Jaws	None	None
	30	Tail, Fins, Brain	Facial Structures, Jaws	None
	50	Tail, Fins	Liver, Somites, Brain	Body Shape, Facial Structures, pharangeal Arches, Jaws
3a	10	Body Shape, Liver, Somites, Notocord,Tail, Fins, Brain,	Heart, Facial Structures, Jaws	None
	30	Body Shape, Notocord,Tail, Brain	Somites, Fins, Heart, Jaws	Facial Structures, Liver
	50	Notocord,Tail, Brain	Body Shape, Somites, Fins, Heart, Jaws	Facial Structures, Liver
3b	10	Body Shape, Liver, Somites, Notocord, Tail, Fins, Brain, Facial Structures, Jaws	None	None
	30	Body Shape, Somites, Notocord, Tail, Fins, Brain, Facial Structures	Liver, Jaws	None
	50	Somites, Notocord, Tail, Fins, Brain, Facial Structures	Body Shape, Fins, Brain, Facial Structures, Jaws	Liver, Heart
3c	10	None	Facial Structures	None
	30	None	Facial Structures	None
	50	Tail, Fins	Body Shape, Facial Structures	None

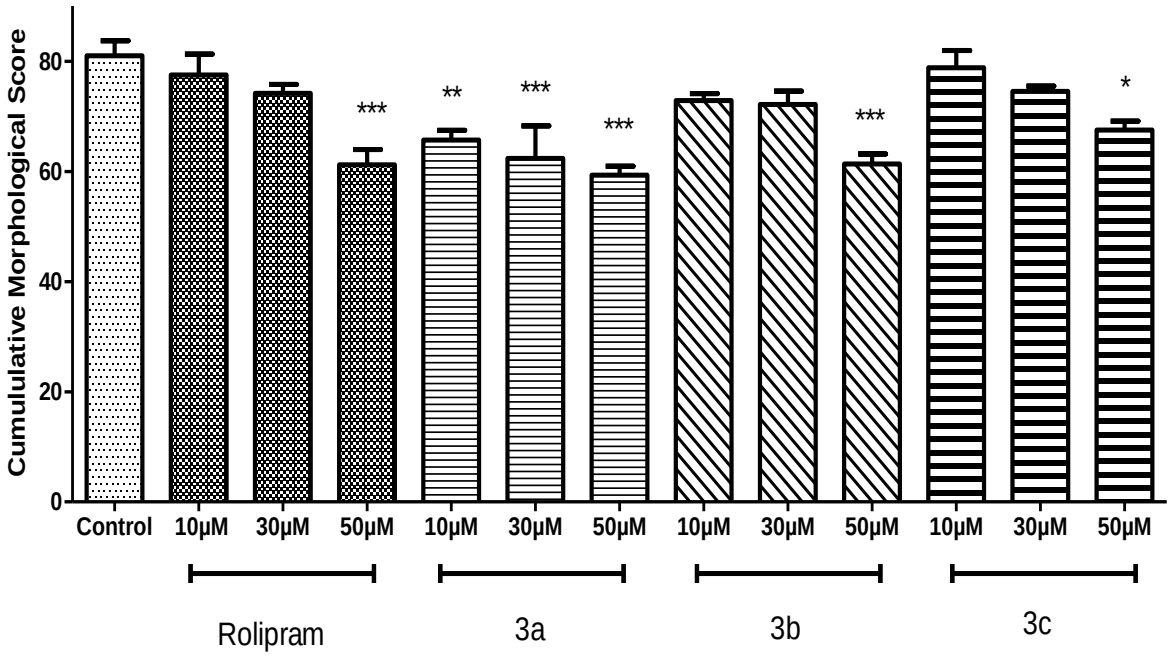

Suppl. Figure 9A. Evaluation of teratogenic effects of compounds in zebrafish embryos. ***, $p<0.0001$; **, $p<0.001$; *, $p<0.05$.

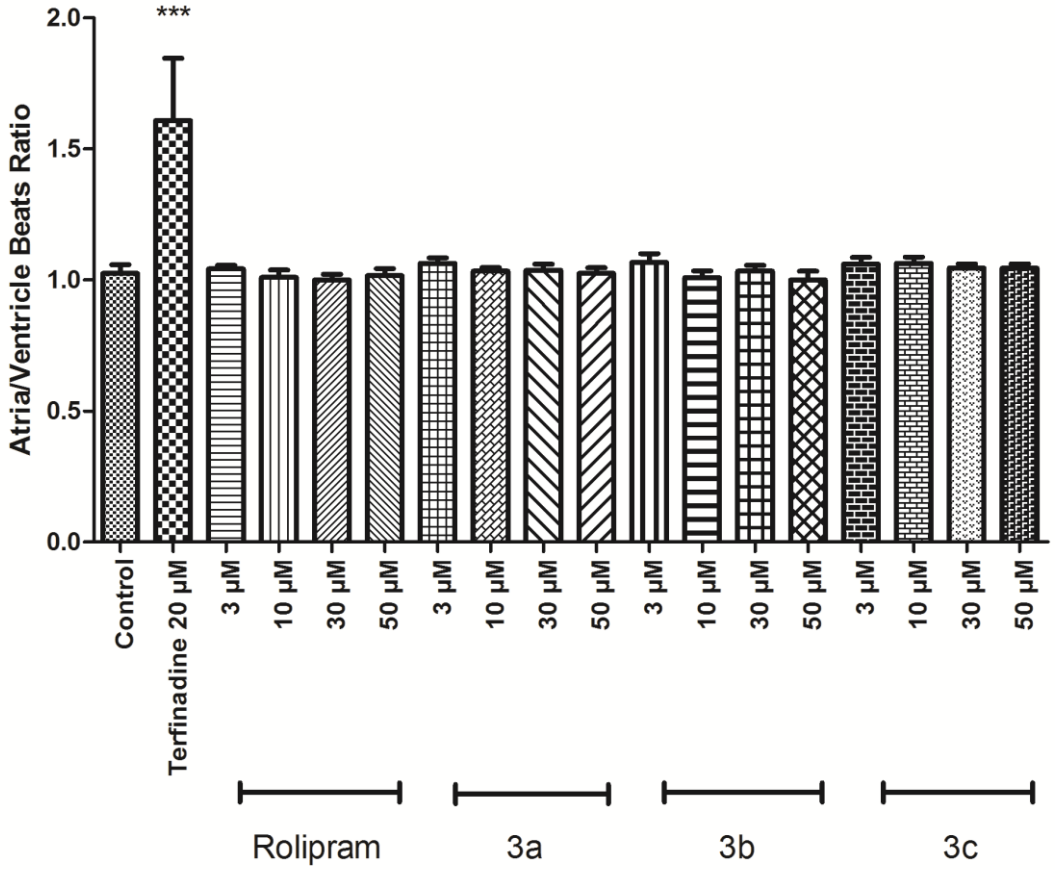

Suppl. Figure 9B. Evaluation of AV beat ratio in 7 day old zebrafish embryos exposed to compounds. ***, $p<0.0001$.

References:

1. Panzica-Kelly J. M., Zhang C. X., Danberry T. L., Flood A., DeLan J. W., K. C. Brannen and K. A. Augustine-Rauch (2010) Morphological Score Assignment Guidelines for the Dechorionated Zebrafish Teratogenicity Assay. *Birth Defects Research* (Part B) 89:382–395 (2010) PMID: 20836125

2. Kimberly C. Brannen, Julieta M. Panzica-Kelly, Tracy L. Danberry, and Karen A. Augustine-Rauch (2010) Development of a Zebrafish Embryo Teratogenicity Assay and Quantitative Prediction Model. *Birth Defects Research* (Part B) 89:66–77 PMID: 20166227.

3. Hill, A. (2011). Hepatotoxicity testing in larval zebrafish. In: McGrath, P. (Ed.), Zebrafish: methods for assessing drug safety and toxicity. West Sussex, UK: Wiley-Balckwell.

4. Milan DJ, Peterson TA, Ruskin JN, Peterson RT, MacRae CA (2003). Drugs that induced repolarization abnormalities cause bradycardia in zebrafish. Circulation 107;1355-1358: PMID: 12642353.

5. Burnouf C and Pruniaux MP (2002). Recent advances in PDE4 inhibitors as immunoregulators and anti inflammatory drugs. Current Pharmaceutical Design 8;1255-1296. PMID: 12052219

Copies of NMR spectra

^{1}H NMR of **4** (400 MHz, $CDCl_3$)

^{1}H NMR (400 MHz, of **3a**

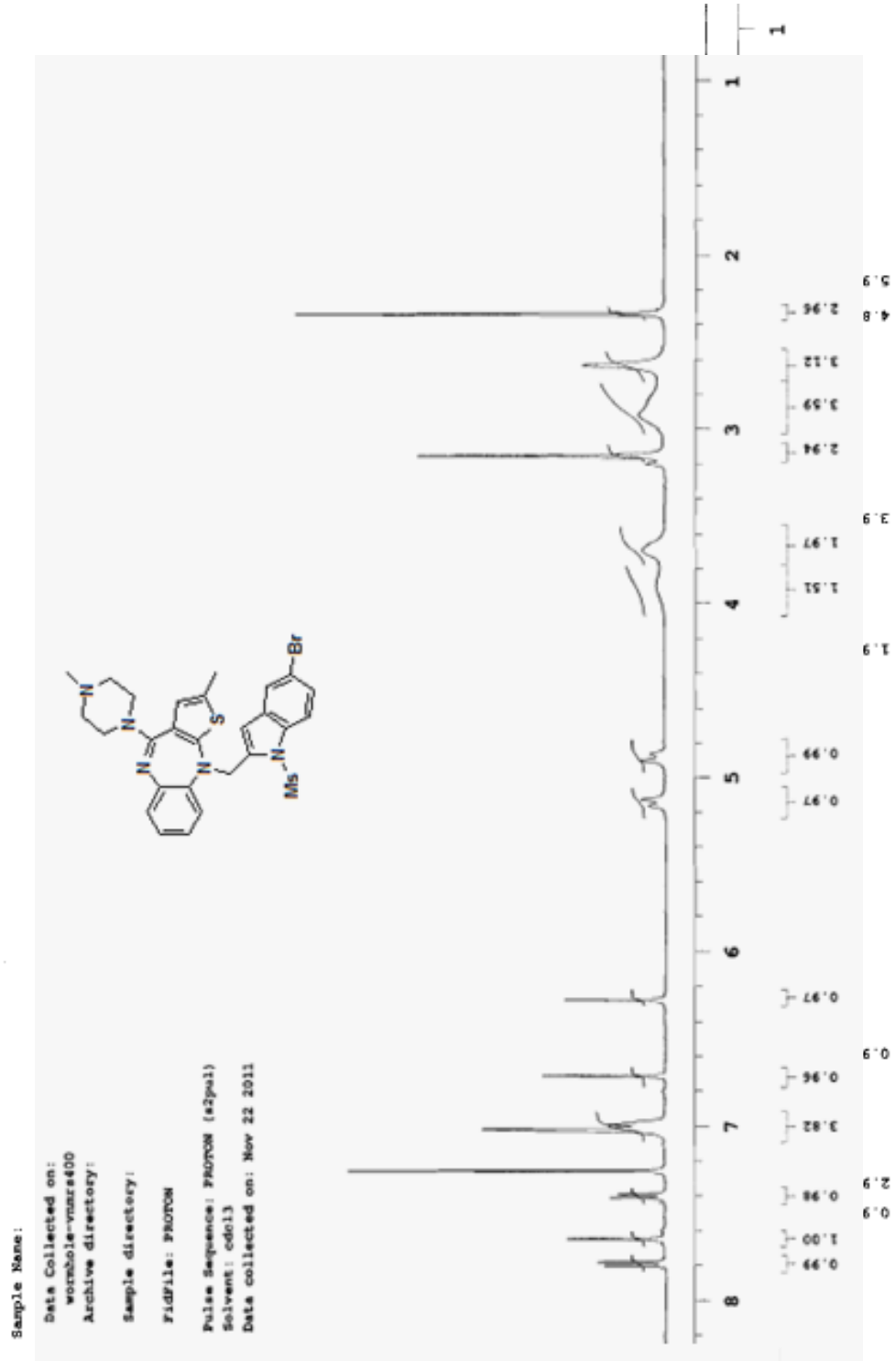

$CDCl_3$)

^{13}C NMR of **3a** (100 MHz, $CDCl_3$)

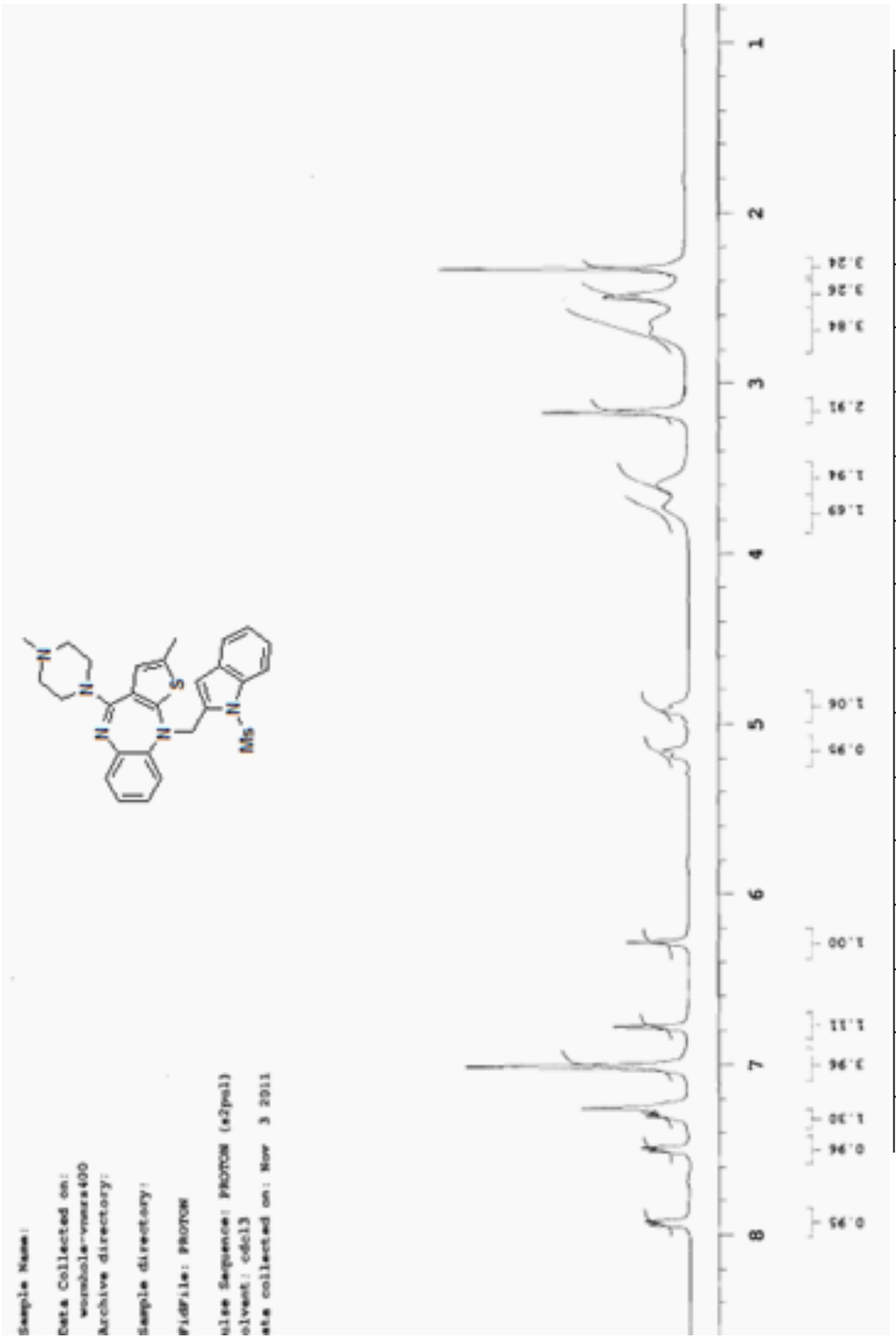

^1H NMR of **3b** (400 MHz, $CDCl_3$)

^{13}C NMR of **3b** (100 MHz, $CDCl_3$)

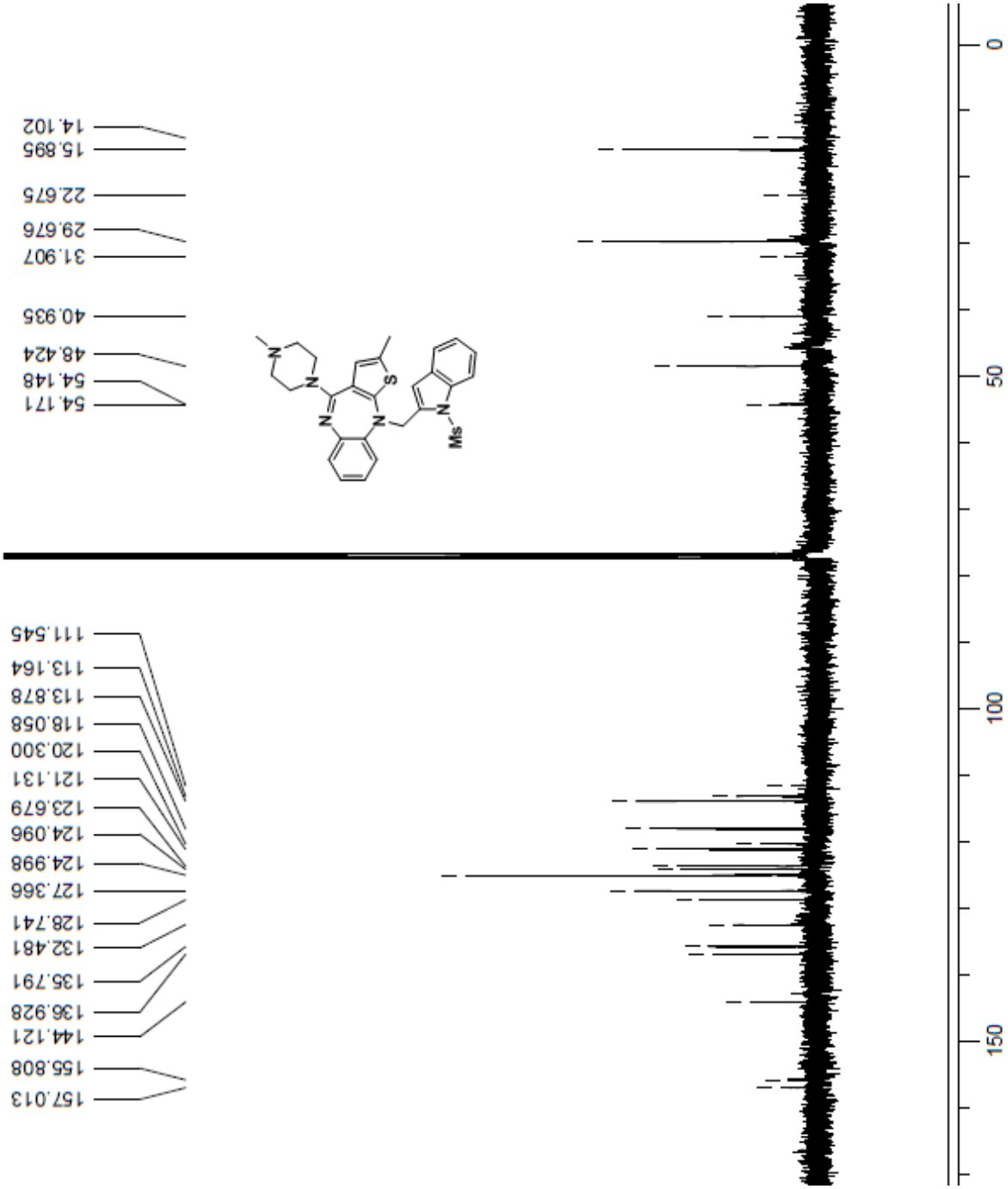

^{1}H NMR of **3c** (400 MHz, $CDCl_3$)

^{13}C NMR of **3c** (100 MHz, $CDCl_3$)

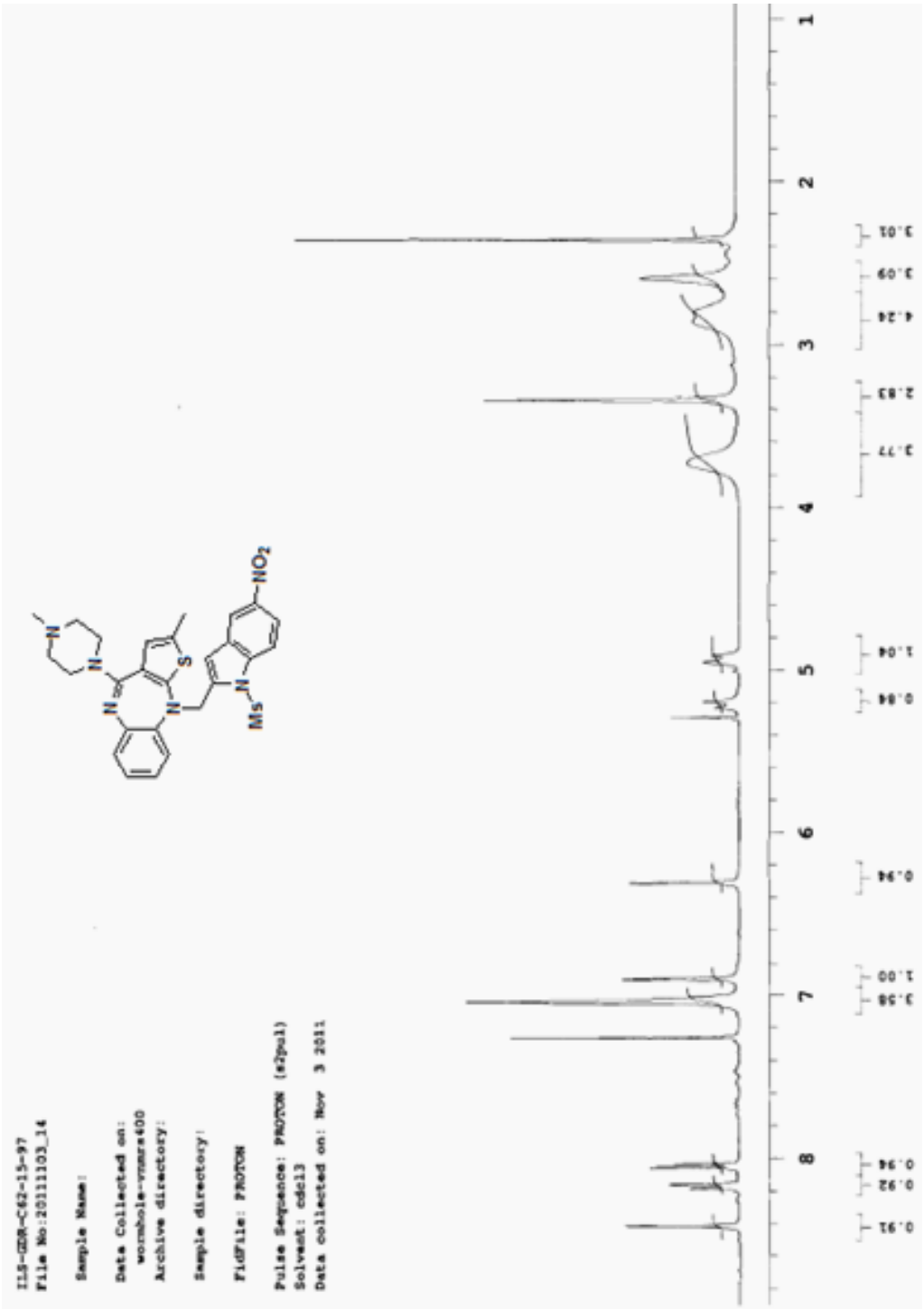

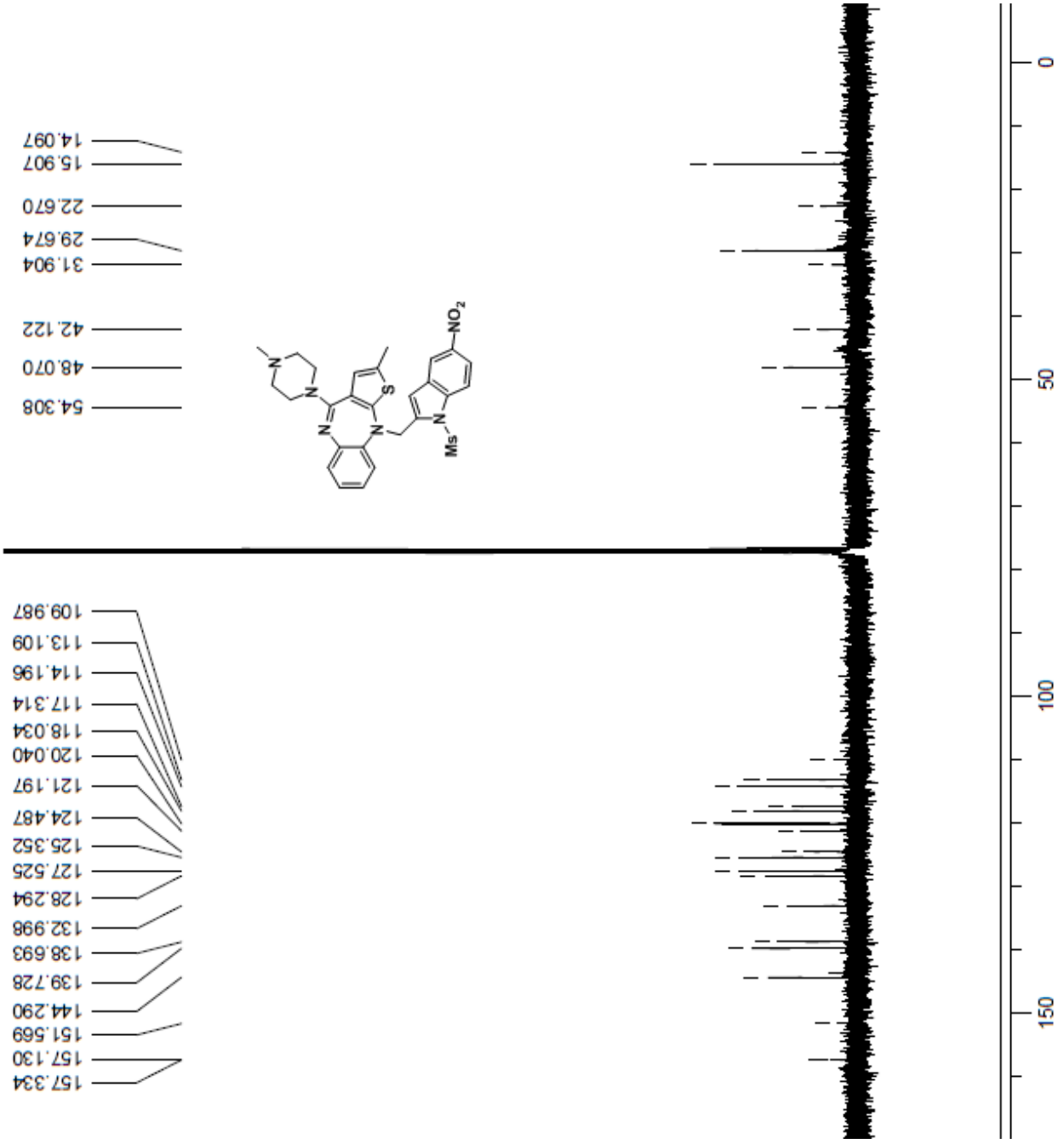

^{1}H NMR of **3d** (400 MHz, $CDCl_3$)

^{13}C NMR of **3d** (100 MHz, $CDCl_3$)

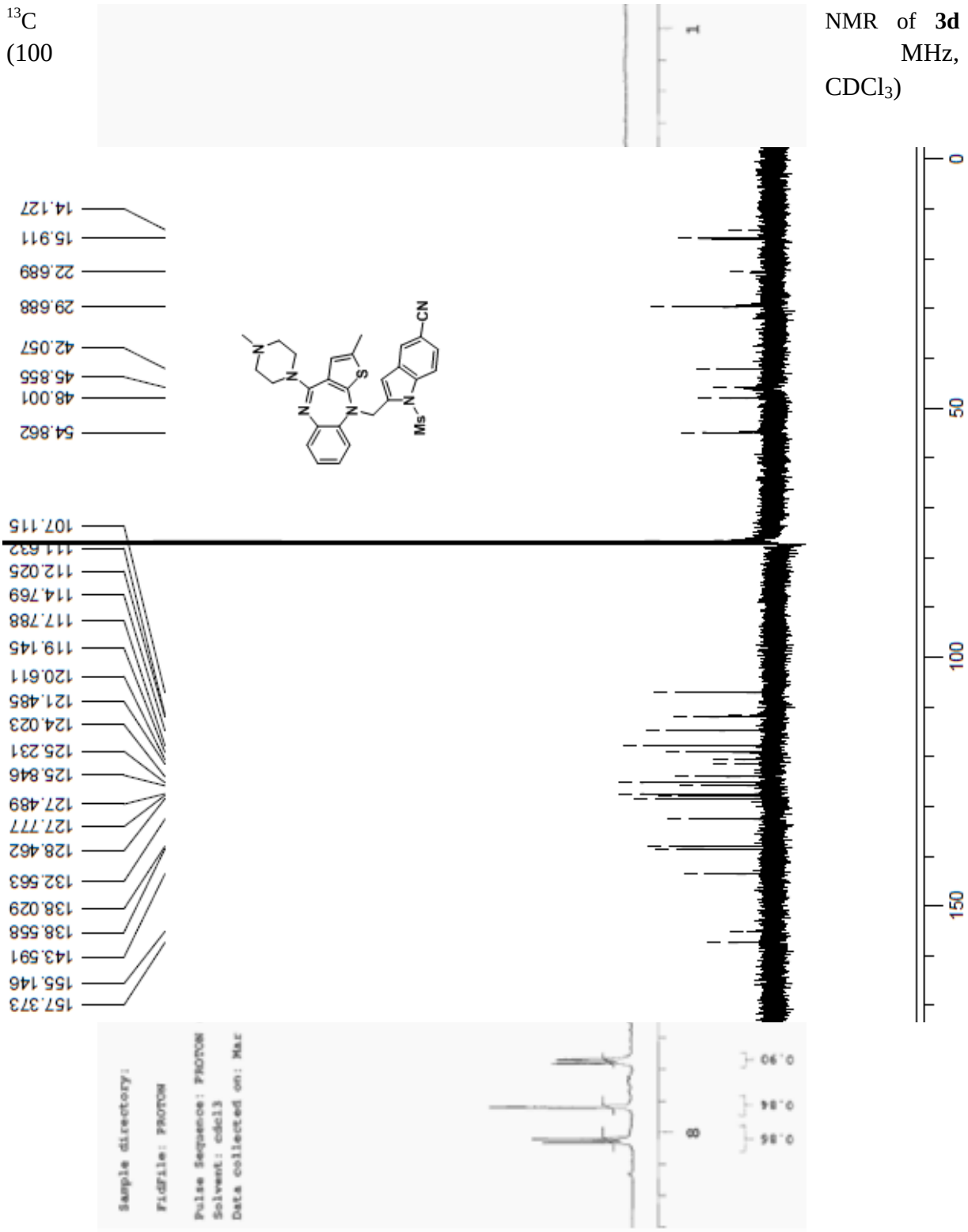

^{1}H NMR of **3e** (400 MHz, $CDCl_3$)

^{13}C NMR of **3e** (100 MHz, $CDCl_3$)

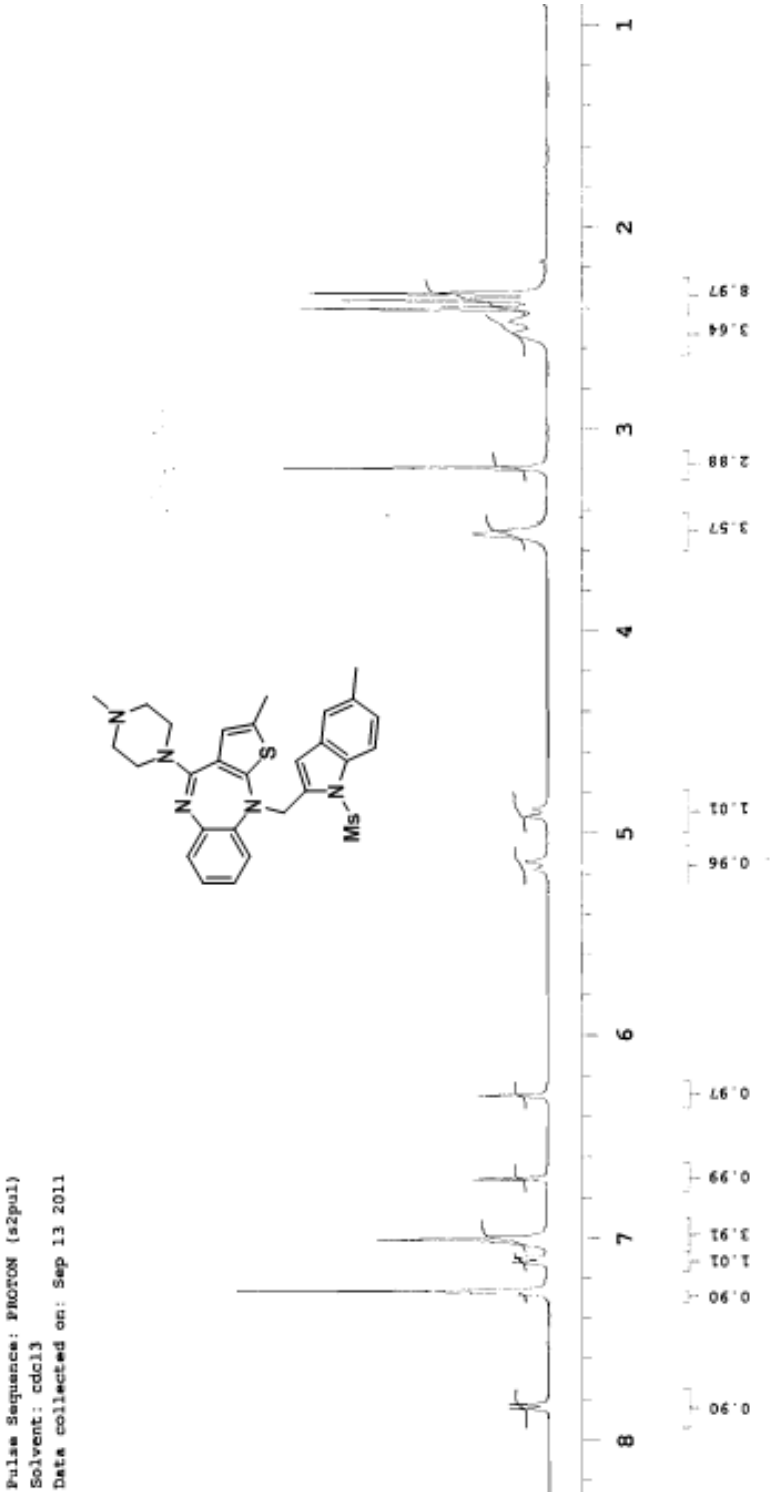

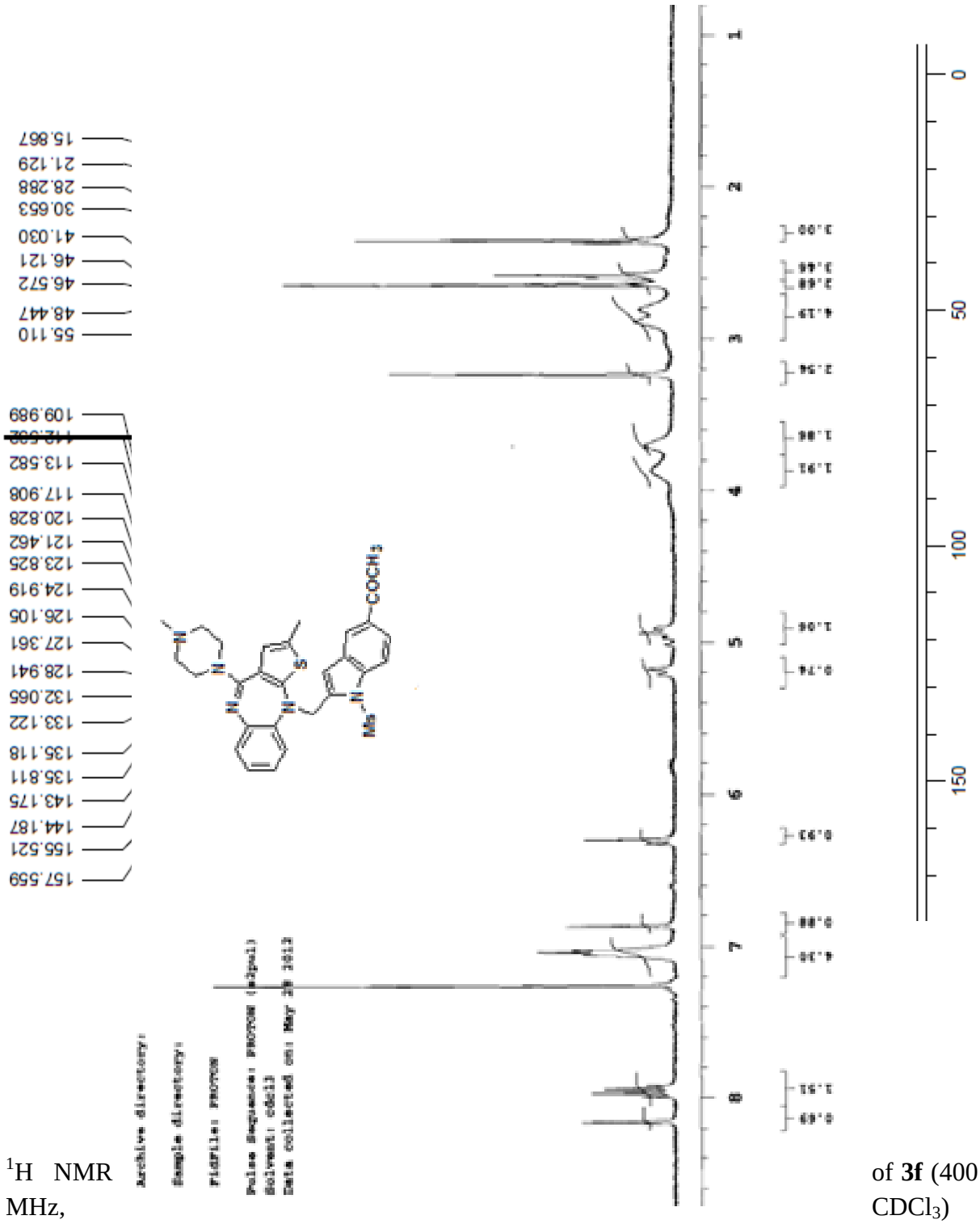

^{1}H NMR of **3f** (400 MHz, $CDCl_3$)

^{13}C NMR of **3f** (100 MHz, $CDCl_3$)

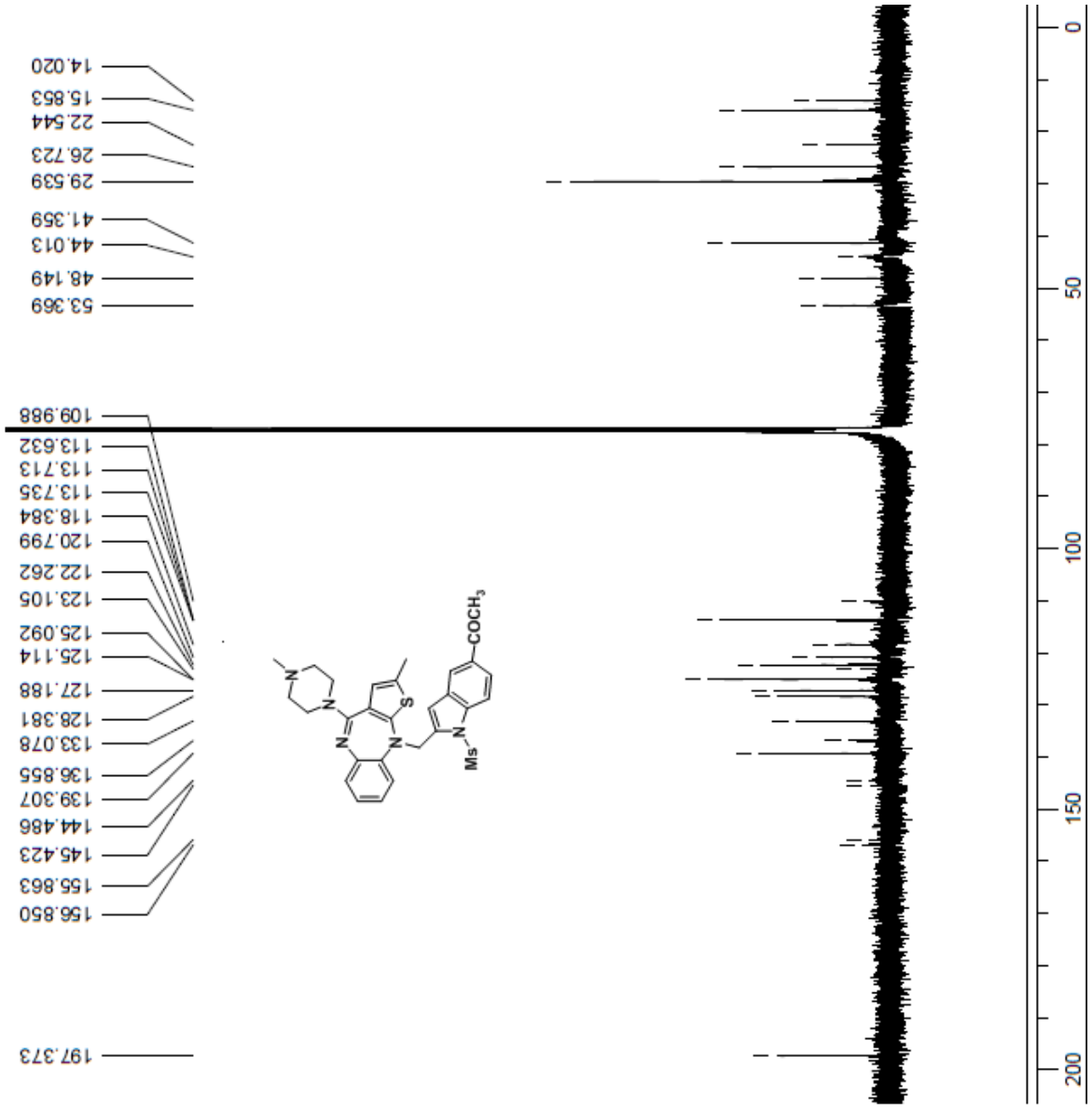

^{1}H NMR (400 MHz, $CDCl_3$) of **3g**

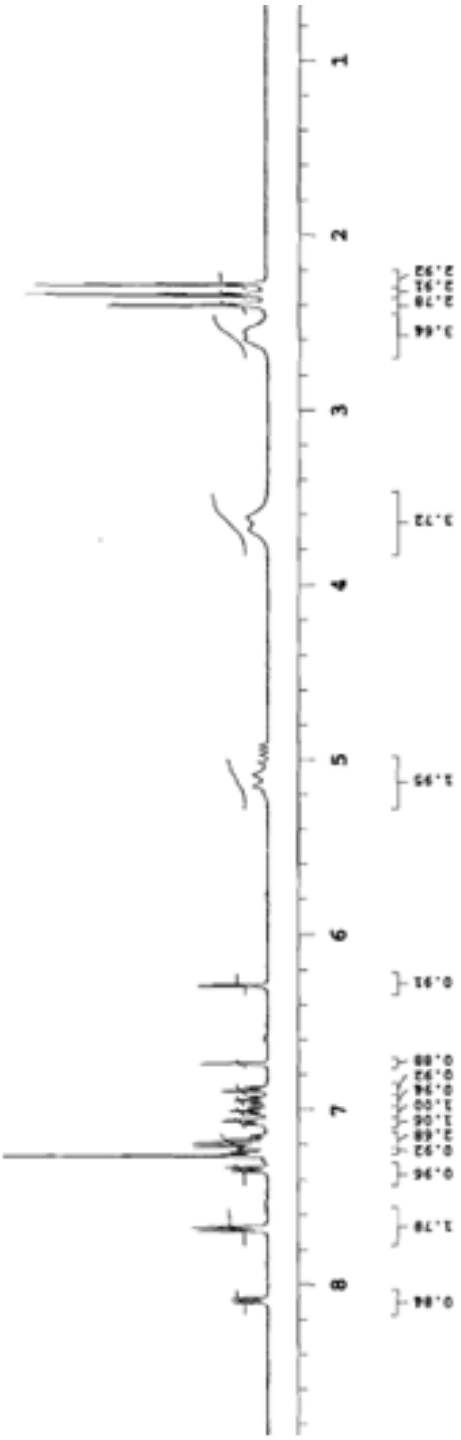

^{13}C NMR (100 MHz, $CDCl_3$) of **3g**

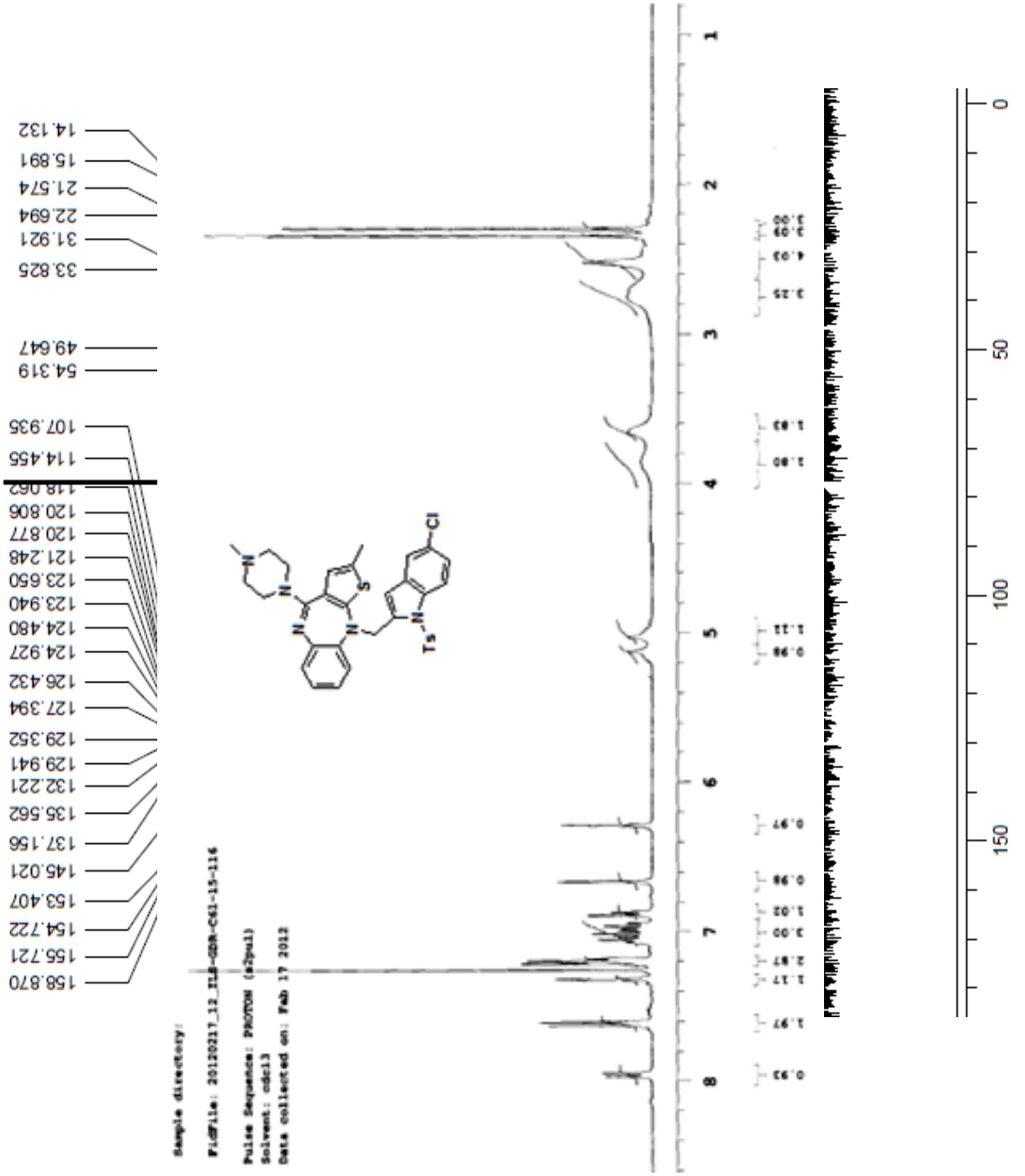

^{1}H NMR of **3h** (400 MHz, $CDCl_3$)

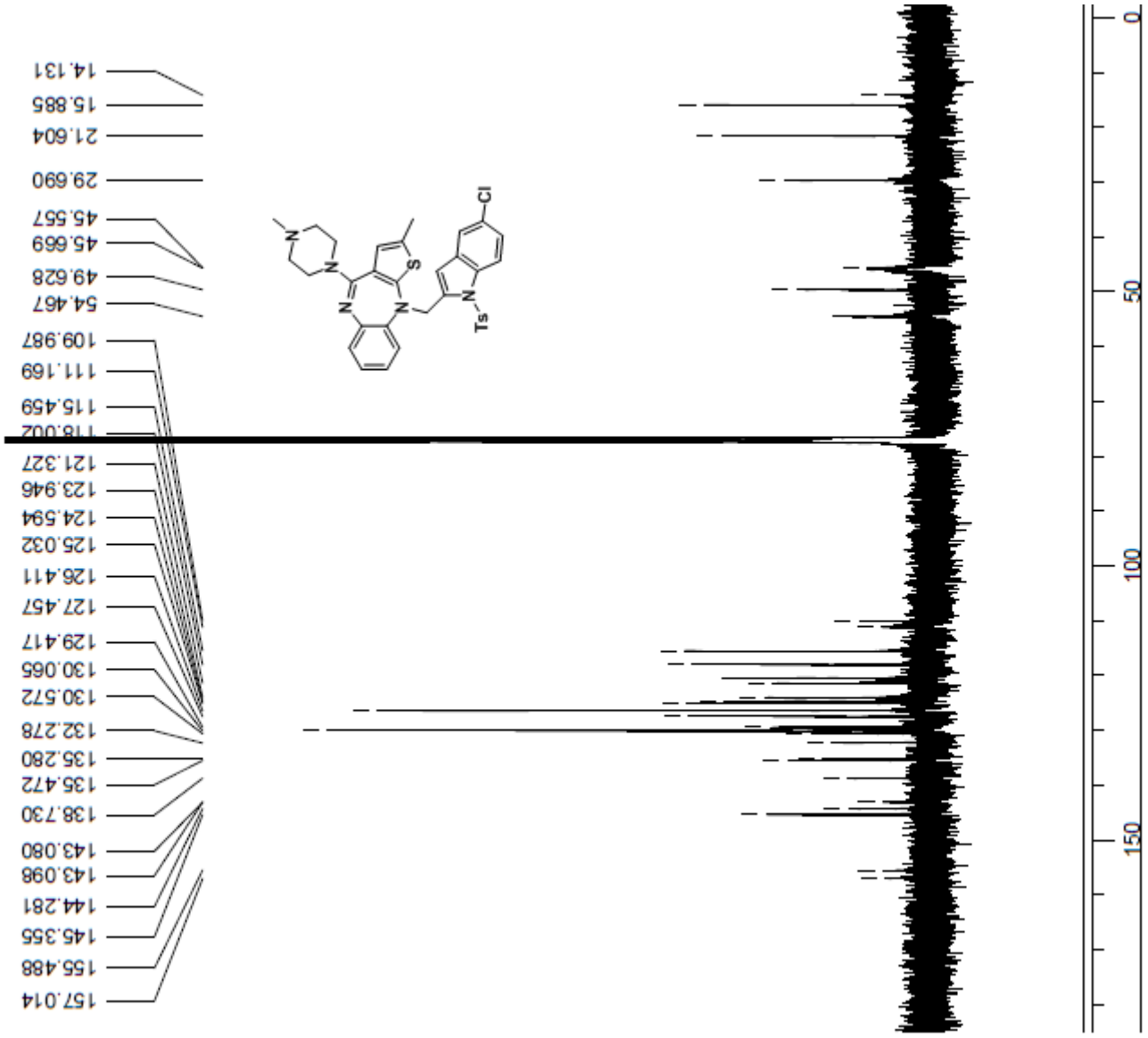

^{13}C NMR of **3h** (100 MHz, $CDCl_3$)

^{1}H NMR of **3i** (400 MHz, $CDCl_3$)

^{13}C NMR of **3i** (100 MHz, $CDCl_3$)

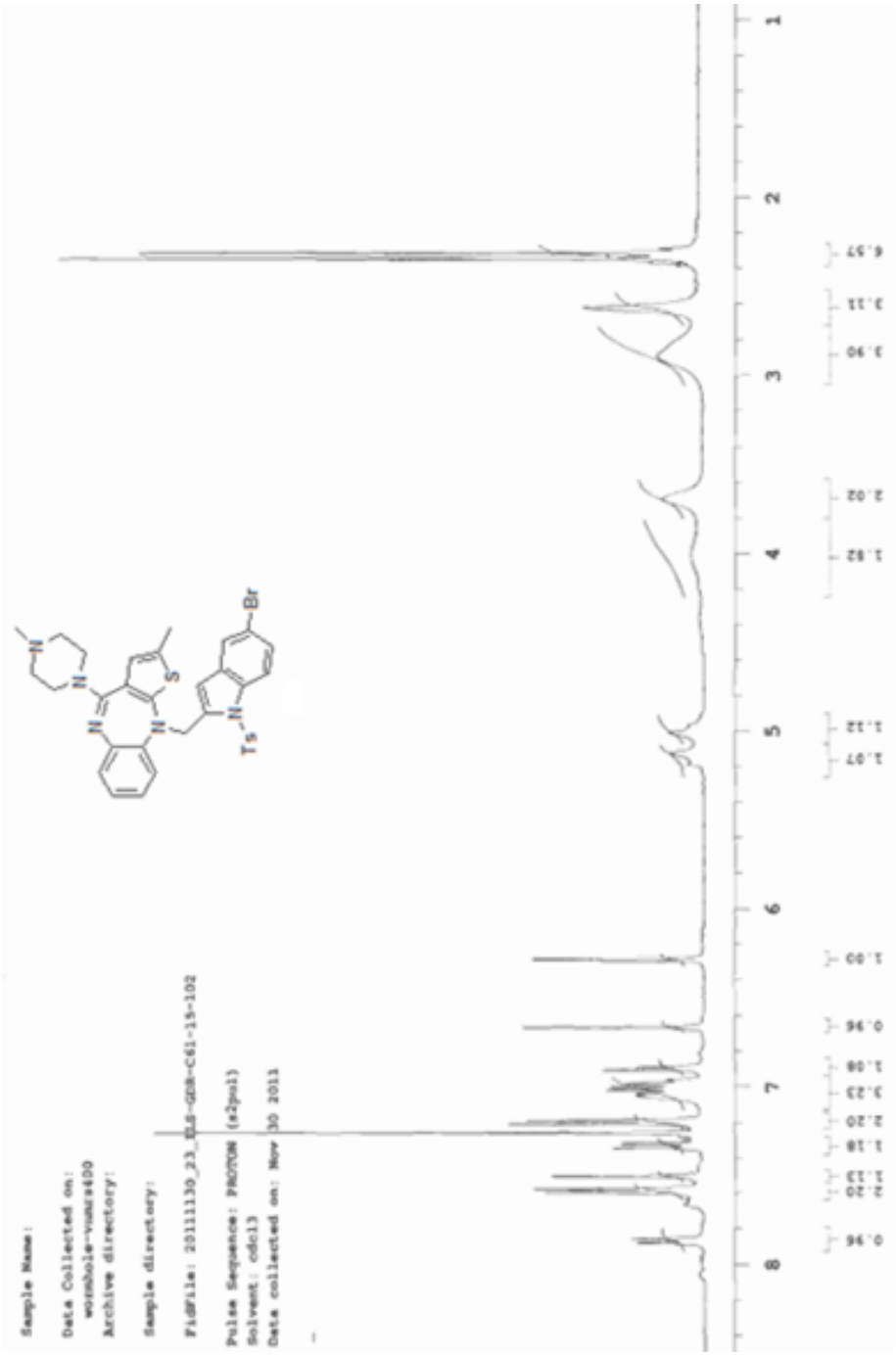

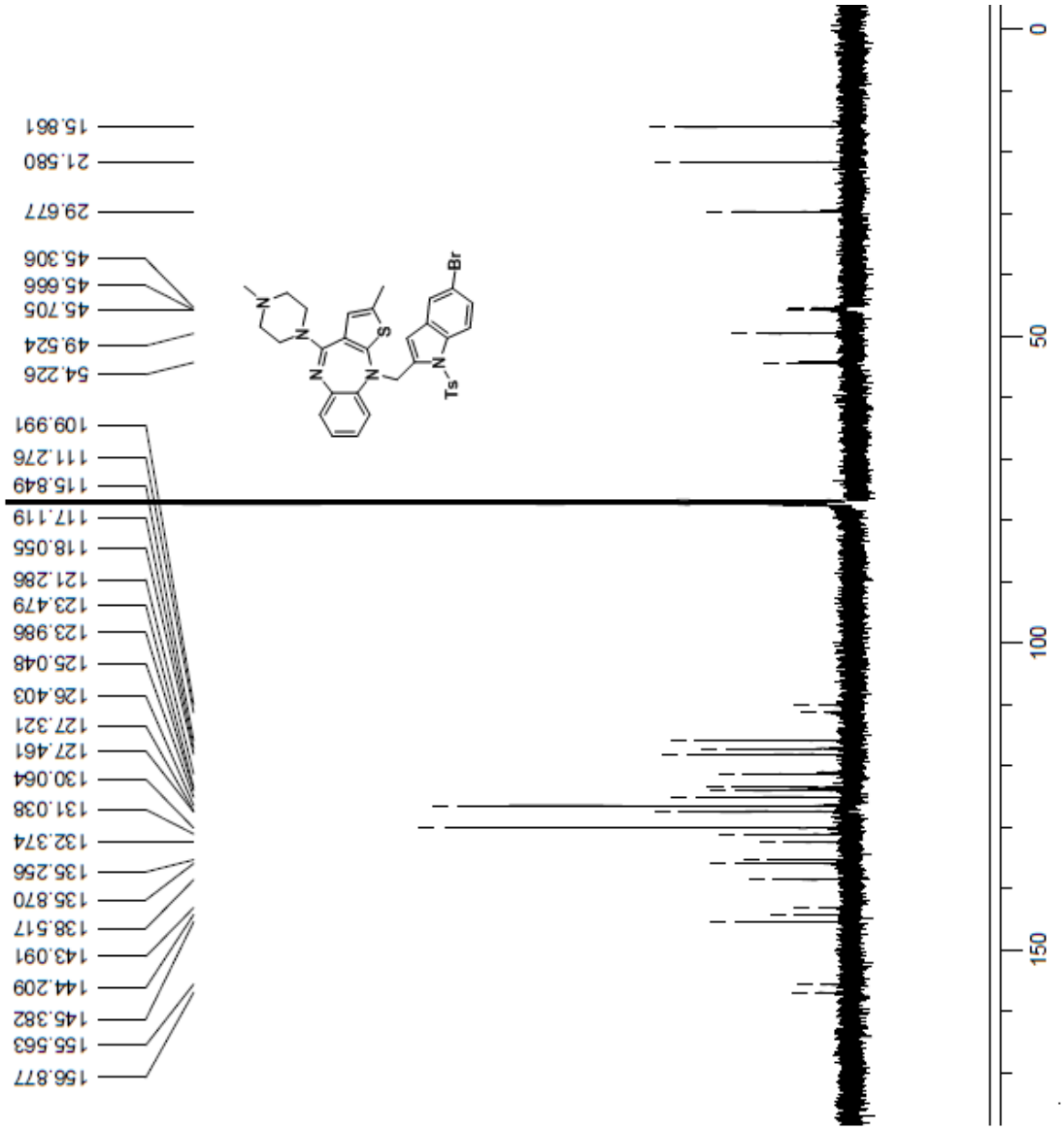

^{1}H NMR of **3j** (400 MHz, $CDCl_3$)

^{13}C NMR of **3j** (100 MHz, $CDCl_3$)